

# Fission yeast Lem2 and Man1 perform fundamental functions of the animal cell nuclear lamina

Yanira Gonzalez,<sup>1</sup> Akira Saito<sup>1</sup> and Shelley Sazer<sup>1,2,\*</sup>

<sup>1</sup>Verna and Marrs McLean Department of Biochemistry and Molecular Biology; Baylor College of Medicine; Houston, TX USA; <sup>2</sup>Department of Molecular and Cellular Biology; Baylor College of Medicine; Houston, TX USA

**Keywords:** fission yeast, HEH domain, LEM domain, nuclear lamina, nuclear periphery, telomere anchoring, chromosome organization

**Abbreviations:** BAF, barrier to autointegration factor; EM, electron microscopy; ER, endoplasmic reticulum; GEF, guanine nucleotide exchange factor; HEH, helix-extension-helix; HEH Domain, HEH-fold containing domain of yeast MSC family proteins; HEH Fold, DNA binding fold, present in LEM domain of higher eukaryotic and HEH domain of yeast MSC family proteins; INM, inner nuclear membrane; LAP, lamin associated protein; LEM, Lap2 Emerin Man1; LEM Domain, HEH-fold containing domain of higher eukaryotic MSC family proteins; MSC, Man1/Src1-C-terminal protein family; NE, nuclear envelope; NPC, nuclear pore complex; SPB, spindle pole body

In animal cells the nuclear lamina, which consists of lamins and lamin-associated proteins, serves several functions: it provides a structural scaffold for the nuclear envelope and tethers proteins and heterochromatin to the nuclear periphery. In yeast, proteins and large heterochromatic domains including telomeres are also peripherally localized, but there is no evidence that yeast have lamins or a fibrous nuclear envelope scaffold. Nonetheless, we found that the Lem2 and Man1 proteins of the fission yeast *Schizosaccharomyces pombe*, evolutionarily distant relatives of the Lap2/Emerin/Man1 (LEM) sub-family of animal cell lamin-associated proteins, perform fundamental functions of the animal cell lamina. These integral inner nuclear membrane localized proteins, with nuclear localized DNA binding Helix-Extension-Helix (HEH) domains, impact nuclear envelope structure and integrity, are essential for the enrichment of telomeres at the nuclear periphery and by means of their HEH domains anchor chromatin, most likely transcriptionally repressed heterochromatin, to the nuclear periphery. These data indicate that the core functions of the nuclear lamina are conserved between fungi and animal cells and can be performed in fission yeast, without lamins or other intermediate filament proteins.

## Introduction

The hallmark of a eukaryotic cell is the nucleus, a specialized region of the endoplasmic reticulum (ER) delineated by the double membranes of the nuclear envelope (NE) (reviewed in refs. 1 and 2). Three possibly interrelated properties that distinguish the nucleus from the ER in all eukaryotes are the flattened sheet conformation of its membranes, the specialized set of inner nuclear membrane (INM) localized proteins, and the sequestration of chromosomes within its confines (reviewed in refs. 2–5). However, fundamental questions about structural and functional differences between the nuclei of higher and lower eukaryotes, including nuclear organization and cell cycle changes in NE area and stability, remain largely unanswered.

These differences are most strikingly seen at mitosis, when animal and plant cells undergo nuclear envelope breakdown (open mitosis) but in most lower eukaryotes, the NE remains intact (closed mitosis) (reviewed in ref. 6). Open mitosis allows the spindle microtubules, which are nucleated by cytoplasmic

localized centrosomes, to physically attach to and then separate the chromosomes. In the closed mitosis of most lower eukaryotes, such as the fission yeast *S. pombe* and the budding yeast *S. cerevisiae*, the centrosome equivalents, named spindle pole bodies (SBPs), are embedded in the NE and nucleate formation of an intra-nuclear spindle<sup>7</sup> (reviewed in ref. 8) that changes nuclear shape as it elongates and separates the chromosomes.<sup>9</sup>

In animal cells, cell cycle dependent changes in NE stability are governed in large part by the nuclear lamina that underlies the INM and forms the structural scaffold for the NE. The nuclear lamina consists of the lamin family of intermediate filament proteins and the transmembrane LAPs (Lamin Associated Protein) that anchor them to the INM. A subset of LAPs have an N-terminal HEH (Helix-Extension-Helix) fold-containing LEM domain (Lap2/Emerin/Man1) that binds to chromatin indirectly by means of its interaction with the non-sequence specific DNA binding protein Barrier to Autointegration Factor (BAF).<sup>10–12</sup> The lamina anchors proteins, heterochromatin and non-transcribed genes to the predominantly transcriptionally

\*Correspondence to: Shelley Sazer; Email: ssazer@bcm.edu  
Submitted: 09/19/11; Revised: 11/19/11; Accepted: 11/22/11  
<http://dx.doi.org/10.4161/nucl.3.1.18824>

repressive environment near the nuclear periphery and provides a structural scaffold for the NE.<sup>2</sup> The critical role of the animal cell lamina for NE structure and chromatin organization is underscored by the observations that mutations in lamins or LAPs cause NE fragility and global changes in gene expression associated with human diseases collectively called laminopathies (reviewed in refs. 13–15). Interestingly, however, lamins are not essential for nuclear envelope structure or proliferation in embryonic stem cells.<sup>16</sup>

During mitosis in all eukaryotes chromatin must dissociate from the NE to allow chromosome condensation and then segregation, but only in the open mitosis of higher eukaryotes is this event accompanied by nuclear envelope breakdown (NEBD). At this point in the cell cycle, phosphorylation of lamina proteins releases them from one another and from the DNA to which they were bound (reviewed in refs. 5, 17 and 18) which destabilizes the NE and releases transcriptionally repressed heterochromatin from the nuclear periphery. Plant cells have evolved a different mechanism to regulate NE stability during open mitosis because although they undergo NE breakdown, they have no lamins, LAPs or BAF.<sup>19,20</sup>

There is growing evidence that the animal cell NE does not break down into vesicles *in vivo* as previously thought, but rather the sheet ER of the NE is reorganized into tubular ER.<sup>1,3,21–23</sup> After mitosis, Man1,<sup>24</sup> and other INM proteins participate in nuclear assembly by re-associating with chromatin and facilitating the conversion of tubular ER into the sheet ER of the reforming the NE.<sup>3,21,23</sup>

Nuclear division during closed mitosis requires a rapid increase in NE area,<sup>25</sup> that, like NE reformation in animal cells,<sup>3,24</sup> depends on restructuring the NE/ER network from tubular to sheet.<sup>26</sup> In fission yeast this mitosis-specific process depends on the Ran GTPase system: in the Ran Guanine Nucleotide Exchange Factor (GEF) temperature sensitive mutant *pim1-d1*, the NE breaks at the time of spindle elongation due to an inability to efficiently convert the tubular ER into the sheet ER of the NE.<sup>26</sup> The Ran GTPase is required for the mitosis-specific NE changes during both closed and open mitosis, however the cellular targets of Ran in these morphologically distinct processes remain unknown<sup>26,27</sup> (reviewed in ref. 2).

Membrane proteins can in principle diffuse throughout the ER/NE membrane system.<sup>28,29</sup> (reviewed in ref. 2), however, their distribution is not random.<sup>30–32</sup> For example, in animal cells the nuclear lamina and proteins with which it interacts are anchored to and enriched specifically at the INM. The basis for the non-random distribution of proteins within the NE/ER membrane and of heterochromatin within the nucleus is less well understood in fungi. Before the *S. cerevisiae* and *S. pombe* genome sequences were known, there was speculation about the presence of a nuclear lamina in yeast; however, no structural or functional orthologs of the nuclear lamins were identified. In the now fully sequenced genomes of *S. cerevisiae*<sup>33</sup> and *S. pombe*<sup>34</sup> there are neither intermediate filament encoding genes nor genes that encode clear orthologs of lamins, LAPs or BAF.<sup>19</sup> However, in their comparative sequence analysis of 28 eukaryotic genomes, using psi-BLAST analysis to identify proteins with distant evolutionary relationships, the Koonin group identified proteins in a variety of

organisms, including yeast, with limited sequence similarity and domain organization characteristic of the animal cell LEM (Lap2, Emerin, Man1) family of LAP proteins (reviewed in ref. 35) and named them MSC (Man1/Src1-C-terminal). Notable is the presence of a conserved N-terminal HEH DNA binding fold within the LEM domain of the animal cell proteins and the HEH domain of yeast proteins. The budding yeast and the fission yeast each have two MSC proteins (named Heh1/Scr1 and Heh2 in *S. cerevisiae* and Lem2 and Man1 in *S. pombe*). It is not clear how proteins, including those responsible for anchoring heterochromatin to the NE, are targeted specifically to the INM in yeast<sup>36,37</sup> although the *S. cerevisiae* Heh1 protein depends on the nucleocytoplasmic transport system for its localization.<sup>28</sup>

In contrast to the genome organization of metazoans in which small heterochromatic domains are interspersed throughout the chromosomes, yeast heterochromatin is predominantly present in the centromere, telomere, rDNA repeats and mating type loci, all of which are enriched at the NE<sup>38</sup> (reviewed in ref. 32). In *S. cerevisiae*, the Heh1/Scr1 protein interacts genetically with transcription export factors, is enriched at the telomere and sub-telomeric loci<sup>39</sup> and anchors rDNA<sup>40</sup> but not telomeres<sup>39</sup> to the nuclear periphery. During interphase, *S. pombe* chromosomes assume the Rabl orientation in which centromeres are anchored at the SPB and telomeres are enriched near the nuclear periphery.<sup>41,42</sup> This telomere anchoring at the NE depends on the telomere-repeat specific constitutive binding protein Taz1, the Taz1-binding protein Rap1, and the INM-associated proteins Bqt3 and the Bqt4.<sup>43</sup> In the absence of Bqt4 the distance of telomeres from the NE increases yet they remain enriched near the nuclear periphery, leading to the suggestion that other proteins may be involved in interphase telomere anchoring *S. pombe*.<sup>43</sup>

We report the characterization of two INM-specific fission yeast transmembrane proteins, Lem2 and Man1, that share limited domain organization and have distant evolutionary relationships but very limited amino acid sequence similarity with the LEM subfamily of animal cell LAPs or the Heh1/Scr1 and Heh2 proteins of *S. cerevisiae*.<sup>19</sup> Like their higher eukaryotic and budding yeast orthologs, fission yeast Lem2 and Man1 localize to the NE; however, Lem2 is unique in its enrichment at the spindle pole body.<sup>44,45</sup> Neither Heh1 nor Heh2 have been reported to influence NE structure or telomere anchoring to the NE but we find that Lem2 and Man1 perform critical functions of the animal cell lamina including anchoring telomeres and other chromatin to the nuclear periphery and contribute to NE structure and stability in the fission yeast *S. pombe* that lacks BAF, lamins and other intermediate filament proteins that are essential components of the nuclear lamina.

## Results

**Identification of Lem2 and Man1 as *S. pombe* proteins that perform some functions of the animal cell lamina.** The starting point of our candidate approach to finding proteins involved in nuclear organization were those shown by the *S. pombe* ORFeome project to localize to the NE<sup>37</sup> that also contained at least one predicted transmembrane domain. We then screened for genes

that, like animal cell lamins,<sup>46,47</sup> altered the conformation of the NE when overexpressed, and then focused on two genes, SPAC14C4.05c and SPAC18G6.10, which met these criteria. Both were also identified<sup>19</sup> as distantly related to the family of animal cell LEM-domain containing proteins (reviewed in ref. 35) (Fig. 1A). Characterization of several members of this protein family indicates a common membrane topology: the N- and C-terminal domains lie in the nucleoplasm and are separated by two transmembrane domains that flank an NE-luminal domain<sup>28,39</sup> that is cysteine-rich in fungi but not metazoans.<sup>19</sup> The N-terminus contains an HEH fold-containing domain (Pfam Clan C10306).<sup>48</sup> The C-terminus contains the winged helix-turn-helix DNA-binding fold-containing Man1/Src1p C-terminal (MSC)<sup>49</sup> domain (Pfam PF09402).<sup>48</sup> Taken together, these data suggest that the proteins encoded by SPAC14C4.05c and SPAC18G6.10 might participate in functions performed by the animal cell nuclear lamina. These *S. pombe* genes are named *man1* (SPAC14C4.05c/*heh2*) and *lem2* (SPAC18G6.10/*heh1*).

**NE structure and integrity depend on Lem2 and Man1.** Null mutants of *lem2* and *man1* ( $\Delta$ lem2 and  $\Delta$ man1) were constructed and tetrad analysis revealed that the mutant spores could germinate and form colonies (Fig. 1B) indicating that neither gene was essential for vegetative growth. The  $\Delta$ lem2 strain was slightly temperature sensitive at 36°C as indicated by the slightly darker pink color of the colony in the presence of the pink vital dye phloxine B, which accumulates in dead cells. The  $\Delta$ lem2 and  $\Delta$ man1 mutations were not synthetically lethal and the temperature sensitivity of the double mutant was similar to that of the  $\Delta$ lem2 strain (Fig. 1C). To determine if Lem2 and/or Man1 influence chromatin organization, DNA in wild type,  $\Delta$ lem2,  $\Delta$ man1, and  $\Delta$ lem2 $\Delta$ man1 cells was visualized with DAPI, but no differences were observed at either 25°C or 36°C (Fig. 1D).

We first assessed the influence of Lem2 and Man1 on NE integrity by visualizing nuclear compartmentation using a previously described fluorescence assay<sup>50</sup> based on monitoring the localization of two exclusively nuclear localized proteins (the NE protein GFP-Nsp1p and the soluble nucleoplasmic protein SV40 NLS-GFP- $\beta$ -galactosidase) that become uniformly distributed in cells when compartmentation is disrupted (Fig. S1A and B). In nearly 100% of wild type,  $\Delta$ lem2,  $\Delta$ man1 and  $\Delta$ lem2 $\Delta$ man1 cells incubated at 25°C or wild type and  $\Delta$ man1 cells at 36°C, both GFP reporters localized exclusively to the nucleus (Fig. 1E; see also Fig. S1C), which is indicative of nuclear compartmentation and normal nucleocytoplasmic transport. Consistent with its slight temperature sensitivity (Fig. 1C), in  $\Delta$ lem2 cells incubated at 36°C nuclear compartmentation was disrupted in  $8.9 \pm 1.8\%$  of cells, whereas deletion of both *lem2* and *man1* ( $\Delta$ lem2 $\Delta$ man1) disrupted compartmentation in  $8.7 \pm 1.0\%$  of cells (Fig. 1E; see also Fig. S1C). Taken together these data indicate that nuclear compartmentation is disrupted in the absence of Lem2 but not Man1.

To confirm that this lack of nuclear compartmentation was caused by loss of NE integrity we examined these strains by transmission electron microscopy (TEM) (Fig. 1F). Consistent with the fluorescence assay results, the NE of  $\Delta$ man1 cells (Fig. 1F, 2) was intact and morphologically similar to that of wild

type cells (Fig. 1F, 1). However, in the absence of *lem2* there were abnormal bulges (Fig. 1F, 3 and 4), indicative of disrupted NE structure, and gaps in the NE (Fig. 1F, 4), indicative of a loss of NE integrity, similar to those in the  $\Delta$ lem2  $\Delta$ man1 double mutant (Fig. 1F, 5 and 6). The distribution of NPCs (nuclear pore complexes) is unaffected by deletion of *lem2*, *man1* or both (Figs. 1F and 6A).

In *S. pombe* the RanGEF, Pim1, is essential for viability and NE integrity.<sup>27</sup> To ask whether *lem2* and/or *man1* function in the *pim1* pathway we examined their genetic interactions with the temperature sensitive *pim1-d1* mutation (Fig. 1E; see also Fig. S1D). Consistent with our previous studies,<sup>26</sup> nuclear compartmentation was intact in 100% of *pim1-d1* cells at 25°C but  $45.2 \pm 2.0\%$  of cells lost compartmentation at 36°C (Fig. 1E). Introduction of the  $\Delta$ man1 mutation did not significantly alter this frequency ( $46.1 \pm 1.1\%$ ) (Fig. 1E; see also Fig. S1D). However,  $97.4 \pm 0.3\%$  of *pim1-d1*  $\Delta$ lem2 cells and  $92.5 \pm 2.3\%$  *pim1-d1*  $\Delta$ lem2  $\Delta$ man1 cells lost nuclear compartmentation after 4hrs at 36°C (Fig. 1E; see also Fig. S1D). These data provide evidence that *pim1-d1* interacts genetically with  $\Delta$ lem2 but not  $\Delta$ man1. The *lem2* null mutation enhances the NE defects in the *pim1-d1* mutation indicating that these genes likely destabilize the NE by distinct mechanisms.

**Lem2 and Man1 localize independently to the NE but only Lem2 accumulates at the SPB.** To confirm the previously described localization of Lem2<sup>44,45</sup> and determine the localization of Man1, each gene at its endogenous chromosomal locus was fused to the gene encoding GFP, causing no change in cell viability (Fig. S2A). Man1-GFP and Lem2-GFP localized exclusively to the NE during all stages of the cell cycle (Fig. 2A, 1 and 3). The chromosomal DNA distribution in these two strains (Fig. 2A, 2 and 4) was the same as that of the negative control wild type cells with no GFP-fusion protein (Fig. 2A, 5).

At this endogenous level of expression Lem2-GFP (Fig. 2A, 1) but not Man1-GFP (Fig. 2A, 3) accumulated in one or two bright spots at or near the NE in most cells (Fig. 2A, 2) in a pattern that resembled that of SPBs in wild type cells,<sup>51</sup> consistent with previous reports.<sup>44,45</sup> The SPB association of Lem2 was confirmed by observing co-localization of Lem2-GFP and the RFP-tagged SPB protein Pcp1<sup>51</sup> in 97% of cells (n = 30) (Fig. 2B). In the absence of Lem2, Man1-GFP remained localized to the NE and in the absence of Man1, Lem2-GFP still localized to the NE and was enriched at the SPB (Fig. 2C), indicating that these two proteins localize to the NE independently of one another. Because of the Lem2 SPB localization, the previously reported interaction of Man1 with the SUN1-domain-containing SPB component Sad1,<sup>52</sup> and the possibility that Lem2 and/or Man1 mediate the interaction between the centromere and SPB, we asked whether either protein influenced the fidelity of chromosome segregation. Following the segregation of Chromosome I as previously described<sup>53</sup> we found no chromosome mis-segregation in  $\Delta$ lem2,  $\Delta$ man1 or wild type cells (n = 100).

**Increased levels of Lem2 or Man1 caused NE membrane proliferation.** Although protein overexpression studies must be interpreted with caution (i.e., overproduction of membrane proteins such as HMG-CoA and animal cell Lamin A and B

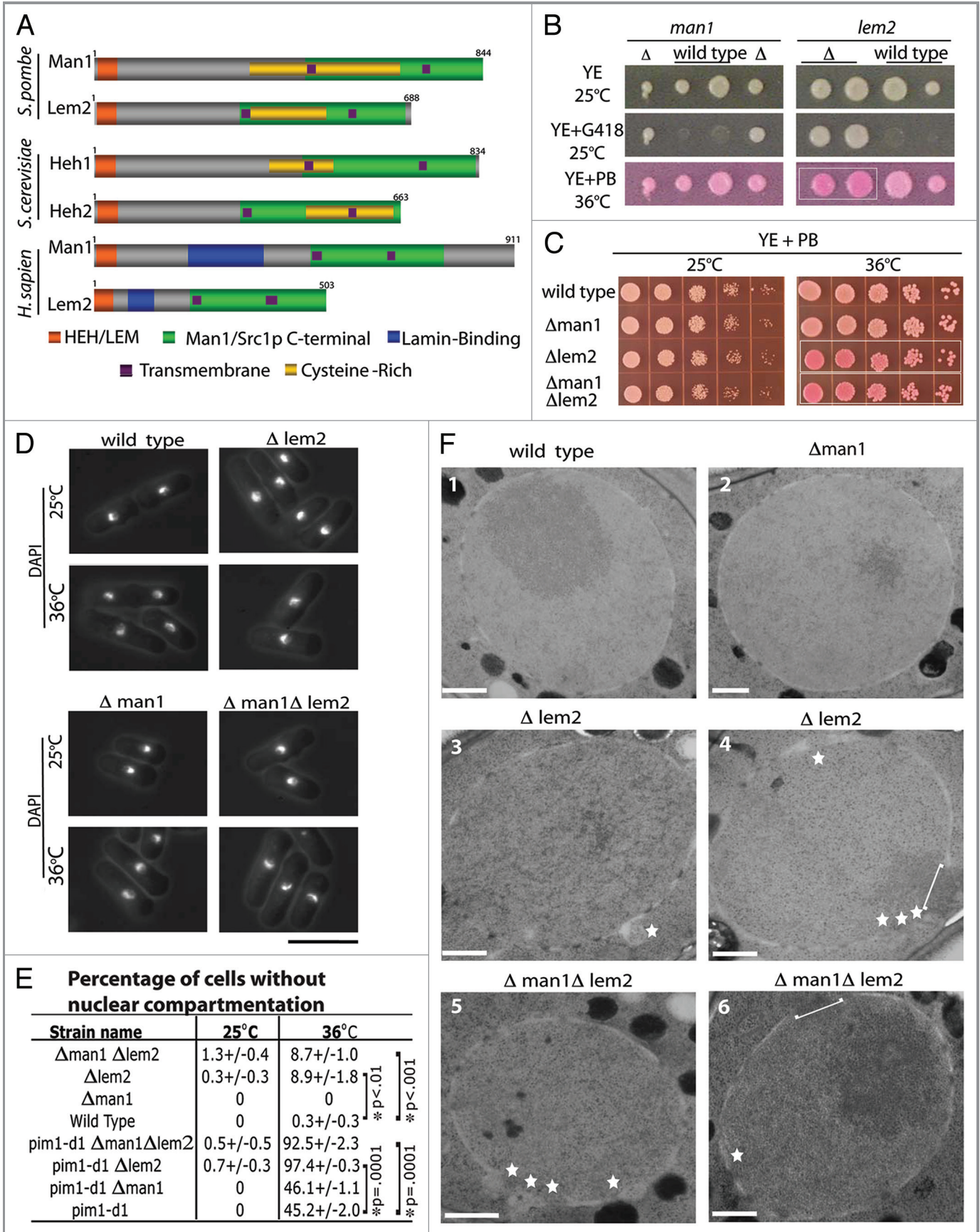


**Figure 1 (See previous page).** Deletion of *man1* or *lem2* does not reduce cell viability or alter chromatin localization but deletion of *lem2* compromises NE integrity. (A) Diagram of the predicted domain structure of Man1/Src1-C-terminal (MSC) family members in *S. pombe* (fission yeast), *S. cerevisiae* (budding yeast) and *H. sapien* (human). This diagram should not be interpreted as implying a correspondence in protein sequence, domain organization or function between specific pairs of proteins (even those with the same name) in different organisms. (B)  $\Delta$ man1,  $\Delta$ lem2 and wild type spores from tetrad analysis were grown on YE at 25°C and replica plated to YE, YE with G418 to identify the null strains or YE with the pink vital dye phloxine B (PB) that accumulates in sick and dead cells turning the colony darker pink, to assess viability and incubated at the indicated temperatures for 2–3 d. White box indicates darker pink colonies. (C) Wild type,  $\Delta$ man1,  $\Delta$ lem2, and  $\Delta$ man1 $\Delta$ lem2 cells were grown in YE to log phase, spotted onto YE + PB plates at 25°C or 36°C and grown for 3–4 d. White box indicates darker pink colonies. (D)  $\Delta$ man1,  $\Delta$ lem2,  $\Delta$ man1 $\Delta$ lem2 cells and wild type cells were grown to log phase at 25°C then incubated at 36°C for 4 h, fixed in ethanol and stained with DAPI to visualize the DNA using fluorescence microscopy. Scale bar = 10 $\mu$ m. (E) Loss of nuclear compartmentation was assayed using a fluorescence-based assay (see Fig. S1) and the percentage of cells in which NE compartmentation is disrupted was determined (n = 200). Asterisk indicates statistically significant difference. (F) Wild type (F1),  $\Delta$ man1 (F2),  $\Delta$ lem2 (F3-F4) and  $\Delta$ man1 $\Delta$ lem2 cells (F5-F6), were high pressure frozen, fixed, stained and visualized using electron microscopy. Star indicates a NE membrane bleb and bracket indicates NE membrane gap. Scale bar = 500nm.

cause proliferation of the ER and the NE respectively<sup>46,47,54</sup>), in the case of Lem2 and Man1 they served three purposes: (1) They demonstrated that Lem2 and Man1 stimulate NE membrane proliferation; (2) they showed that Lem2 and Man1 influence NE conformation in morphologically different ways suggesting that they are functionally and/or structurally different in their membrane interactions; and (3) most importantly, they provided an experimental system in which to characterize the putative DNA binding ability of Lem2 and Man1. When overexpressed in the nuclear compartmentation reporter strain background<sup>50</sup> (Fig. S1A), no vector control containing cells but 15.2% of *lem2* cells and 12.9% of *man1* cells (n = 300) lost nuclear compartmentation, compared with 0% of wild type cells (Fig. 3A). Overexpression of neither *lem2* nor *man1* influenced NPC distribution but they did cause some of the NPC component GFP-Nsp1 to accumulate in the ER at the cell periphery (Fig. 3A, 5) that is continuous with the NE<sup>26,55</sup> and co-localized with a fluorescent ER reporter (unpublished observations). In addition, 35.0% of *man1* cells had what appeared to be GFP-containing spherical structures in the cytoplasm (Fig. 3A, 3) with GFP-Nsp1 localized to their periphery (Fig. 3A, 6). Overexpression of either *man1* or *lem2* in wild type cells was toxic (Fig. S2B). For this reason, all overexpression studies were performed by first growing cells to log phase with the *nmt1* gene promoter off, then turning the promoter on and monitoring the consequent phenotypes.

When Lem2-YFP was overproduced for 30 h, the protein localized to the nuclear interior in very brightly fluorescent curvilinear or circular patterns (Fig. 3B, 1). Using identical conditions, overproduced Man1-YFP localized to the periphery of spherical cytoplasmic structures and accumulated in the peripheral ER (Fig. 3B, 2). To determine whether these were NE-derived membranes we investigated their protein composition. Man1-GFP and Lem2-GFP expressed from their endogenous promoters localize to the nuclear periphery as previously shown (Fig. 2A, 1 and 3). However, both localized to the periphery of the cytoplasmic spheres and/or the intranuclear membrane stacks induced by overexpression of either untagged *man1* or untagged *lem2* (Fig. S3) which are similar in morphology to the membranes seen upon overexpression of fluorescently tagged proteins (Fig. 3B). These data indicate that the protein composition of the membranes that form upon *lem2* or *man1* overexpression are similar to that of the NE, and that Lem2 and Man1 do not compete with one another for membrane association.

To determine if the localization of overexpressed Man1-YFP and Lem2-YFP corresponded to an underlying sub-cellular structure, cells were examined using transmission electron microscopy. In contrast to wild type cells (Fig. 3C, 1), cells overexpressing *lem2* had multi-layered stacked membrane structures at the nuclear periphery (Fig. 3C, 2) and in spheres and swirls within the nucleus (Fig. 3C, 3 and 4), continuous with or derived from the inner NE. Overexpression of *man1* also resulted in the appearance of some stacked membrane structures within the nucleus (Fig. 3D, 1 and 2). However, only *man1* overexpression caused the formation of small cytoplasmic nucleus-like spheres attached to the nucleus, that had double lipid bilayer membranes (Fig. 3D, 1–4) and structures resembling nuclear pores (Fig. 3D, 4), both characteristic of the NE. It is for these reasons we refer to these small spheres as tethered “mini-nuclei.” These data indicate that overproduction of either Lem2 or Man1 protein caused distinct morphological changes in the NE and that the protein composition resembles that of the NE from which they are derived.

**DNA co-localized with the nuclear membranes that proliferated upon overexpression of Lem2 or Man1.** These overproduction studies provided the basis for an experimental system in which to examine the roles of Lem2 and Man1 in anchoring chromatin to the NE. In cells overproducing Lem2-YFP, DNA localization was strikingly altered from that of wild type cells (compare Fig. 4A, 1 and 3 with Fig. 2A, 5) and co-localized with Lem2p-YFP on the intranuclear NE membranes (Fig. 4A, 1). The DNA in Man1-YFP overproducing cells co-localized with the protein at the periphery of the nucleus and at the periphery of the mini-nuclei (Fig. 4A, 4). Imaging of control cells lacking either the YFP-fusion protein (Fig. 4A, 3 and 6) or the DAPI dye (Fig. 4A, 2 and 4) confirmed that the signals in Figure 4A, 1 and 4 reflect co-localization.

The membrane of the nucleus and the membrane of the mini-nuclei were continuous (Fig. 4B). The presence of DNA in these mini-nuclei and in the connections among them and between them and the nucleus (Fig. 4B) indicates that they are derived from the nucleus and are the product of deformation of both the inner and outer nuclear membranes. Taken together these data indicate that overexpression of Lem2 or Man1 deforms the NE in morphologically different ways and that these two proteins directly or indirectly anchor chromatin to the NE membrane.

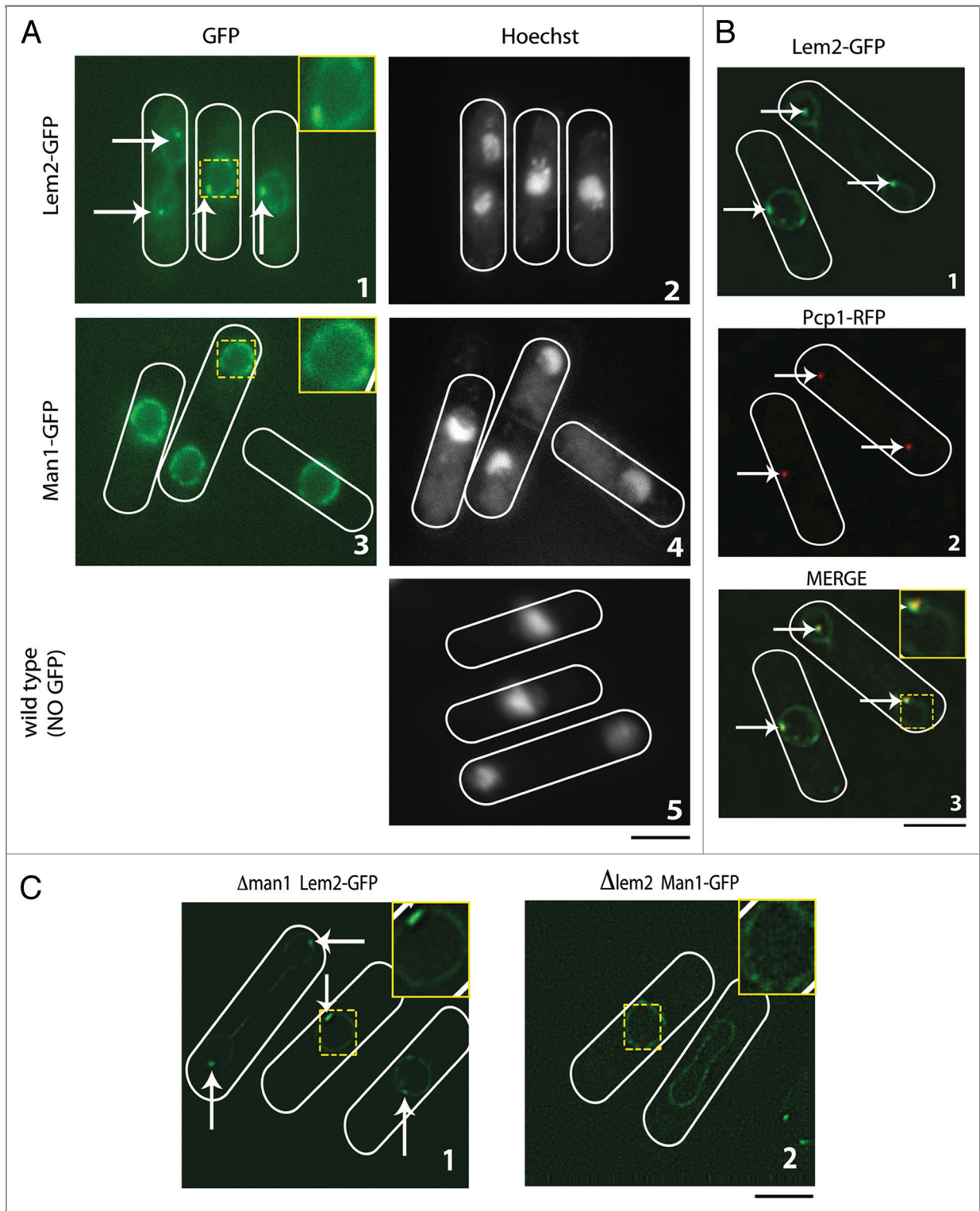


**Figure 2.** Endogenously expressed Man1-GFP and Lem2-GFP localize to the NE independently of one another and Lem2 accumulates at the SPB. Wild type cells with endogenously produced Lem2-GFP (A1, A2), Man1-GFP (A3, A4), or wild type control cells with no GFP-tagged protein (A5) were grown in YE to log phase at 25°C and live cells were stained with the DNA-binding dye Hoescht 33342. The protein (GFP) and DNA (Hoescht) localization were monitored in live cells by deconvolution microscopy. Arrow indicates Lem2-GFP NE localized foci. (B) Cells with endogenously produced Lem2-GFP and the SPB reporter Pcp1-RFP were grown to log phase at 25°C. Protein localization was monitored in live cells. Arrow indicates Lem2 and Pcp1 co-localization. (C)  $\Delta$ man1 cells with endogenously produced Lem2-GFP (C-1) or  $\Delta$ lem2 cells with endogenously produced Man1-GFP (C-2) were grown to log phase at 25°C and protein localization was monitored in live cells. Scale Bar = 5 $\mu$ m. Boxed insets are twice the size of the original image.

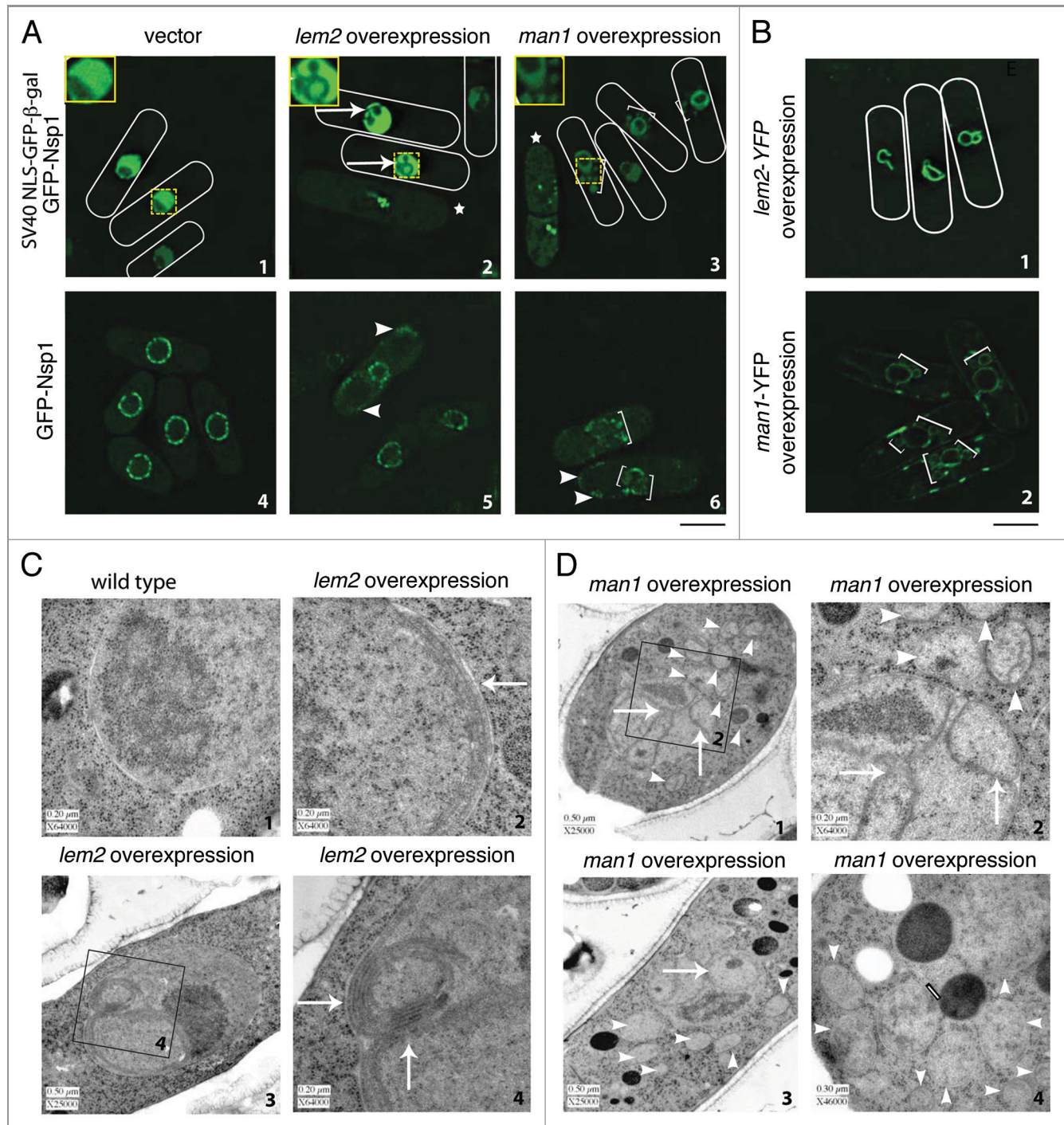


**Figure 3.** Overexpression of *man1* or *lem2* disrupts NE integrity and alters nuclear membrane structure. Expression of *lem2* or *man1* from the *nmt1* gene promoter in plasmid pREP3X or an empty vector control was repressed and the cells grown to log phase, then derepressed for 30 h at 25°C. (A-1, A-2, A-3) Expression in cells with the nucleoplasmic reporter SV40 NLS-GFP-β-gal and the NE reporter GFP-Nsp1. Nuclear compartmentation was monitored in live cells. Star indicates cell without nuclear compartmentation; arrow indicates GFP-excluding nuclear structure; bracket indicates GFP-containing cytoplasmic spheres. Cell outlines are shown in white. (A-4, A-5, A-6) Expression in cells with only GFP-Nsp1. Protein localization was monitored in live cells. Arrowhead indicates GFP-Nsp1 at the cell periphery; bracket indicates GFP-Nsp1 at the periphery of cytoplasmic spheres. Scale bar = 5 μm. Boxed insets are twice the size of the original image. (B) Expression in wild type cells, of (B-1) *lem2*-YFP or (B-2) *man1*-YFP from the *nmt1* gene promoter in an integrated pDUAL plasmid, was derepressed for 30 h at 25°C, and protein localization was monitored in live cells. Brackets indicate cytoplasmic spheres. Cell outlines are shown in white. Scale bar = 5 μm. (C) Wild type cells (C1) or wild type cells in which expression of *lem2* (C2, C3, C4) or *man1* (D1 to D4) from the *nmt1* gene promoter in pREP3X was derepressed for 30 h at 25°C were high pressure frozen, fixed, stained and visualized using electron microscopy. Arrow indicates intranuclear membrane stack; arrowhead indicates cytoplasmic membrane-bound spheres; black and white bar indicates NPC-like structure. Scale bars are as indicated on individual panels.

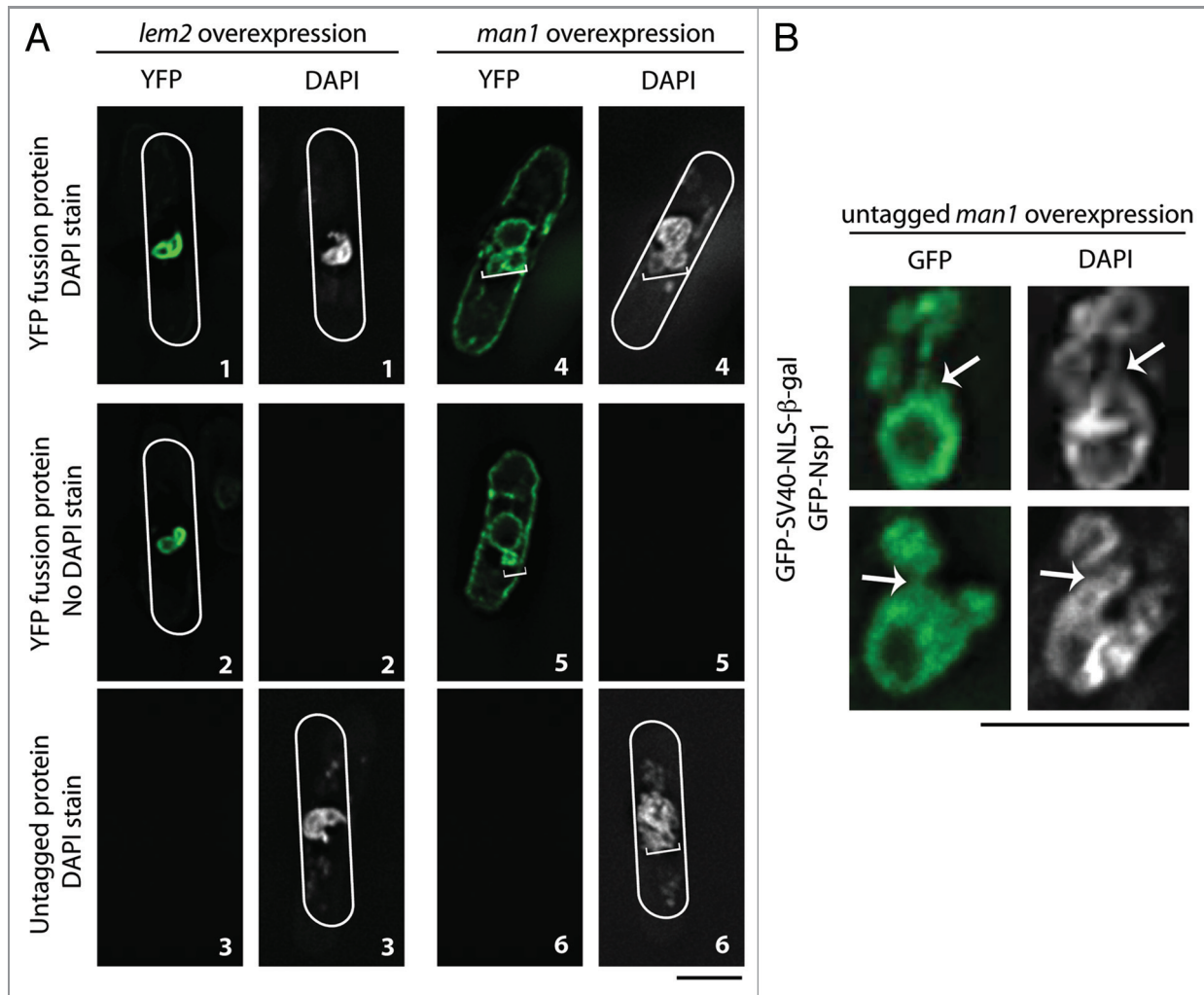


**Figure 4.** DNA Co-localizes with overexpressed Man1p or Lem2p. Expression in wild type cells, of *lem2*-YFP (A-1, A-2, A-3) or *man1*-YFP (A-4, A-5, A-6) from the *nmt1* gene promoter in an integrated pDUAL plasmid, was derepressed for 30 h at 25°C. Cells were fixed with methanol, stained with DAPI and protein and DNA localization monitored. To ensure that the observed co-localization was not due to visualization of one fluorophore with the microscope filter set of the other, cells with only the YFP fusion protein but no DAPI stain (A2, A5) or cells overexpressing the untagged version of each protein stained with DAPI (A3, A6) were included as negative controls. Bracket indicates mini-nuclei. Cell outlines are shown in white. Scale bar = 5 μm. (B) Expression in cells with SV40 NLS-GFP-β-gal and GFP-Nsp1 of untagged *man1* from the *nmt1* gene promoter in pREP3X was derepressed for 30 h at 25°C. Cells were fixed with methanol, stained with DAPI, and protein and DNA localization monitored. Arrow indicates connection between the nucleus and mini-nucleus. Scale bar = 5 μm.

DNA co-localization with Lem2 or Man1 was dependent on the HEH domain and overexpression of the HEH domain alone caused chromosome hyper-compaction. To ask if the influence of Lem2 or Man1 on chromatin depended on the putative DNA-binding HEH domain, truncated versions of Man1-YFP or Lem2-YFP lacking the HEH domain (Man1<sup>ΔHEH</sup>-YFP or Lem2<sup>ΔHEH</sup>-YFP respectively) (See Fig. 1A) were overexpressed in wild type cells. Protein localization and DNA morphology (Fig. 5A) were compared with those of cells overexpressing the full-length proteins (Fig. 4A) or expressing the proteins from their respective endogenous promoters (Fig. 2A). A small proportion of full length and truncated Man1-YFP and truncated Lem2 localize to the ER at the cell periphery. ER localized full length Lem2-YFP cannot be clearly visualized, in part because of the very strong fluorescence

signal from the stacked NE membranes. Lem2<sup>ΔHEH</sup>-YFP and Man1<sup>ΔHEH</sup>-YFP proteins had the same NE association as their full-length counterparts, although the morphology of the proliferated membrane was somewhat different when visualized by fluorescence microscopy (compare Fig. 4A and Fig. 3B to Fig. 5A) and electron microscopy (compare Fig. 5B, 1 and 2 with Fig. 3C, 2–4; compare Fig. 5B, 3 with Fig. 3D, 1–4). In contrast to their full-length versions (Fig. 4A, 1 and 4), DNA did not co-localize with overexpressed Lem2<sup>ΔHEH</sup>-YFP or overexpressed Man1<sup>ΔHEH</sup>-YFP at the periphery of the nucleus (Fig. 5A, 2 and 4). Because protein gel blot analysis showed that the levels of full-length and truncated proteins are similar (data not shown), these data show that the influence of Lem2 and Man1 on the NE and chromatin anchoring were dependent on their respective HEH domains and not to differences in protein levels.

In an alternative approach to determining the *in vivo* function of the HEH domain of Man1 and Lem2 (HEH<sup>Man1</sup>, HEH<sup>Lem2</sup>) (see Fig. 1A), each domain or the vector control was overexpressed in wild type cells and the DNA visualized using DAPI (Fig. 5C, 1–3). This led to a striking hypercompaction of the chromosomes in 72.0% of cells with HEH<sup>Lem2</sup>, 12.0% with HEH<sup>Man1</sup> but 0% with the vector control (n = 200). The proportion of binucleated cells in the vector control, HEH<sup>Lem2</sup> or HEH<sup>Man1</sup> overexpressing strains was similar (13.0%, 8.9% and 10.4% respectively, n = 200) indicating that cell cycle progression was not effected. Overexpression of HEH<sup>Lem2</sup>, HEH<sup>Man1</sup>, or vector control in cells with the nuclear pore protein Nup107-RFP showed that the compacted DNA localized to a single focus at the NE (Fig. 5C, 4–6). Overexpression of HEH<sup>Lem2</sup>, HEH<sup>Man1</sup>, or the vector control in cells with the SPB protein Sid4-GFP<sup>56</sup> revealed that the hypercompacted DNA foci co-localized with the SPB in 96% of HEH<sup>Man1</sup> cells and 98% of HEH<sup>Lem2</sup> cells (n = 200) (Fig. 5C, 7–9)

**Lem2 and Man1 are required for anchoring of telomeres at the nuclear periphery.** To ask whether Lem2 or Man1 participate in telomere anchoring, we monitored the intranuclear position of the telomere-binding protein Taz1-GFP<sup>57</sup> with respect to the nuclear periphery delineated by the nuclear pore complex (NPC) protein Nup107-RFP in wild type and null mutant strains (Fig. 6A). Using a previously described method,<sup>58</sup> the relative position of each telomere with respect to the nuclear diameter was used to assign it to one of three zones of equal area within an optical section of the nucleus: Zone I at the periphery, Zone II near the periphery and Zone III in the middle (Fig. 6B). If telomeres were randomly positioned in the nucleus, equal proportions of telomere spots would be found in each zone, but that was not the case in wild type cells: 64% of telomeres were found in zone I, 20% in zone II and 16% in zone III, a distribution skewed toward the nuclear periphery and significantly different from random (p < 0.0001) (Fig. 6C). The distribution of telomeres into the three zones was significantly different from the distribution in wild type cells for both the  $\Delta$ lem2 and  $\Delta$ man1 strains (p < 0.0001, p < 0.0002 respectively). The percentage of telomeres at the nuclear periphery decreased to 47.9% in the  $\Delta$ lem2 strain, (Fig. 6D) and to 57.8% in the  $\Delta$ man1 strain (Fig. 6E). Telomere distribution in the absence of both Lem2 and Man1 was also significantly different from that of wild type cells (p < 0.0002) but did not differ from that of  $\Delta$ lem2 (p > 0.1) indicating that the defects caused by the  $\Delta$ lem2 and  $\Delta$ man1 mutations are not additive.

## Discussion

Despite substantial differences in nuclear structure and organization between higher and lower eukaryotes, we find that *S. pombe* Lem2 and Man1, INM localized proteins distantly related to the animal cell LEM-domain containing subfamily of LAPs, perform essential functions of the animal cell nuclear lamina. Although yeast undergo closed mitosis and lack the animal cell BAF protein, that mediates the interaction of LEM proteins with chromatin, and the lamin intermediate filament protein, that is a key

component of the animal cell nuclear scaffold, we show that these two fission yeast proteins influence NE structure and integrity, anchor chromatin to the NE via their HEH-domains, and are previously unknown components of the telomere anchoring system.

**Lem2 and Man1 are integral proteins of the INM with nuclear N-terminal DNA-binding HEH domains.** Previous characterization of several members of the LEM-domain protein family<sup>15,39,44,45</sup> indicates that they are integral INM proteins with two transmembrane domains and N- and C-terminal DNA-binding nucleoplasmic domains. Our data, showing that Lem2 and Man1 localize to the NE to which they bind and anchor chromatin through their N-terminal HEH-domains, are consistent with this predicted membrane topology.

**Lem2 and Man1 influence NE structure.** In animal cells the LEM protein Man1 is important for changing ER conformation from tubular to sheet form during NE reformation after mitosis.<sup>24</sup> This is consistent with our observation that overexpression of either Lem2 or Man1 causes the formation of sheet membrane stacks in the NE. A similar but not identical proliferation of membrane is seen when lamins are overproduced in animal cells<sup>46,51</sup> or when vertebrate lamin B receptor is overexpressed in human<sup>59</sup> or budding yeast cells.<sup>60</sup> Overexpression of the *S. cerevisiae* protein Src1/Heh1 or Heh2 also changes chromatin organization, but alteration of NE organization was not reported.<sup>61</sup> The Man1 induced tethered “mini-nuclei” in *S. pombe* are morphologically distinct from the nuclear blebs seen in animal cells with mutant lamins,<sup>62,63</sup> the DNA-free nuclear protrusions (flares) in budding yeast cells<sup>64</sup> or the nuclear morphology of budding yeast cells overexpressing the INM-associated protein Esc1.<sup>61</sup>

It has recently been shown that the luminal domain of *S. cerevisiae* Src/Heh1 but not Heh2 interacts with the membrane-associated nucleoporin Pom152p and in certain mutant backgrounds influences NPC distribution in the NE and causes nucleoporin mislocalization to the cytoplasm.<sup>65</sup> In contrast, mutation of neither Lem2 nor Man1 influences NPC distribution or function, although they do have the fungal-specific cysteine-rich luminal domain that is similar in amino-acid composition but not sequence to that of the *S. cerevisiae* Heh1 and Heh2 proteins.<sup>19</sup>

**NE integrity depends on Lem2.** In *S. pombe*, the NE remains intact throughout the cell cycle, and we show that Lem2 is essential for this nuclear compartmentation. The NE gaps in  $\Delta$ lem2 cells likely result from destabilization of the NE at the sites of NE lumen dilation. These data suggest the possibility that Lem2 may directly or indirectly interact with proteins in the NE lumen or the ONM (Outer Nuclear Membrane) that tether the two membranes to each other and/or maintain the uniform spacing of the INM and ONM. In cells with NE gaps, the spherical structure of the nucleus is maintained, a morphology similar to that seen when a transient NE hole arises from a defect in SPB insertion into the membrane.<sup>66</sup> But, it is strikingly different from the morphology of cells lacking a functional Ran-GTPase system<sup>27,67</sup> in which the NE fragments due to its inability to sufficiently increase NE area during elongation of the

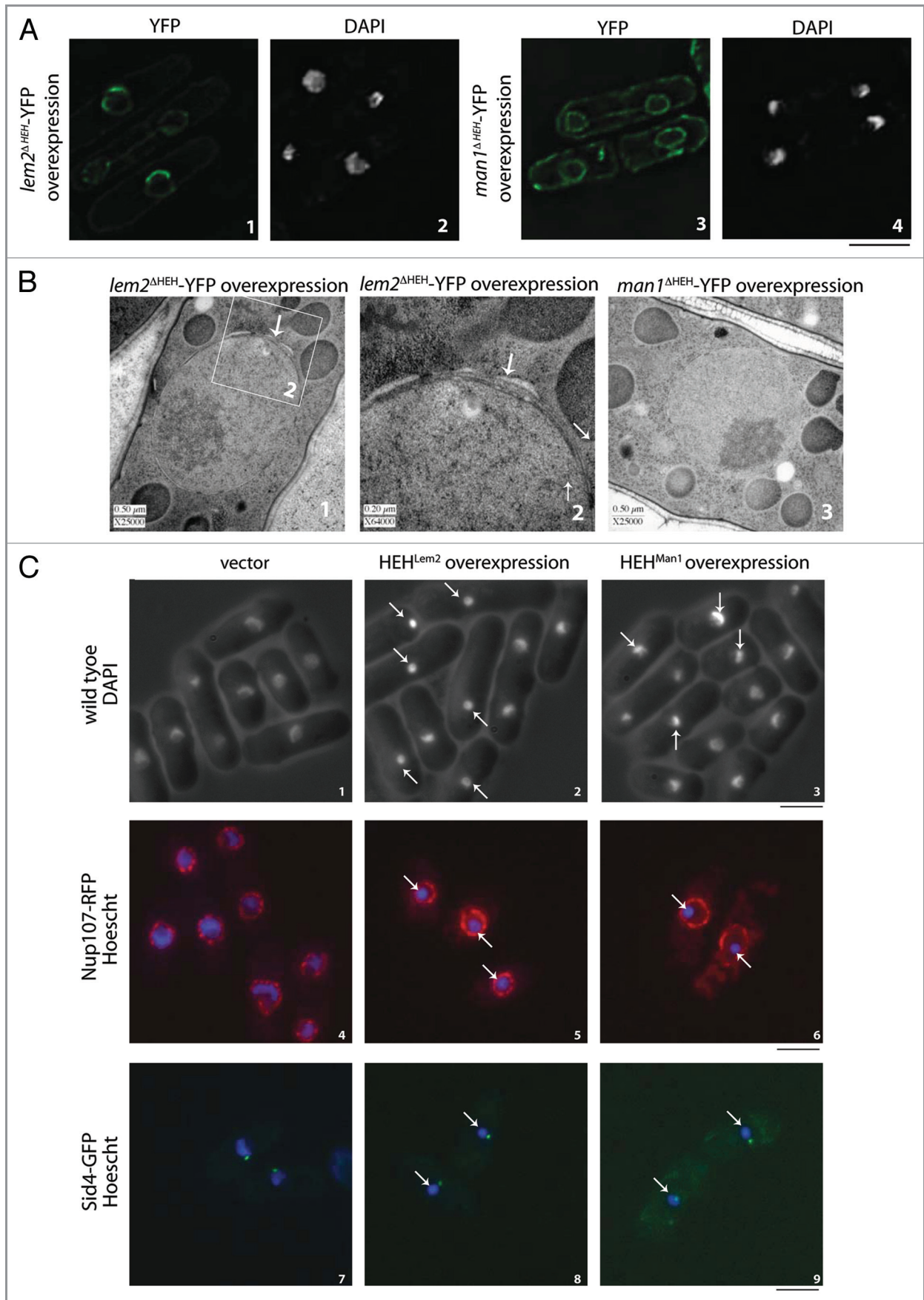


**Figure 5 (See previous page).** The HEH domain was necessary for co-localization of overexpressed *lem2* or *man1* with chromatin and overexpression of the HEH domain caused compaction of SPB-tethered chromatin. (A and B) Expression in wild type cells, of *lem2* or *man1* lacking the HEH domain ( $\Delta$ HEH) and tagged with YFP (*lem2* <sup>$\Delta$ HEH</sup>-YFP or *man1* <sup>$\Delta$ HEH</sup>-YFP respectively) from the *nmt1* gene promoter in an integrated pDUAL plasmid, was derepressed for 30 h at 25°C. (A) Cells were fixed with methanol and stained with DAPI. Protein (YFP) and DNA (DAPI) localization were monitored. Scale bar = 5  $\mu$ m. (B) Cells were high pressure frozen, fixed, stained and visualized using electron microscopy. Arrow indicates membrane stack. Scale bars are as indicated on individual panels. (C) Expression of the HEH domain of *lem2* (HEH<sup>*lem2*</sup>) (C-2, C-5, C-8) or *man1* (HEH<sup>*man1*</sup>) (C-3, C-6, C-9) from the *nmt1* gene promoter in plasmid pDS473a, or an empty vector control (C-1, C-4, C-7), was derepressed for 30 h at 25°C in wild type cells (C-1, C-2, C-3), in cells with the NPC localized protein Nup107-RFP (C4, C5, C6), or in cells with the SPB-localized protein Sid4-GFP (C7, C8, C9). Cells were fixed in ethanol (C1, C2, C3) and the DNA visualized with DAPI using fluorescence microscopy or the DNA in live cells was visualized with Hoechst 33342 (C4-C9) and examined using deconvolution microscopy. Arrow indicates hyper-compacted DNA. Scale bar = 5  $\mu$ m.

intranuclear spindle. We find that *lem2* but not *man1* interacts genetically with the temperature sensitive Ran GEF *pim1-d1* mutant and significantly exacerbates its previously characterized NE defects, suggesting that they influence the NE by independent mechanisms. In contrast, deletion of *man1* does not destabilize the NE either alone or in combination with the  $\Delta$ *lem2* or *pim1-d1* temperature sensitive mutations.

Localization to the INM of the *S. cerevisiae* HEH-domain proteins Heh1 and Heh2 requires Ran GTPase dependent nuclear protein import,<sup>28</sup> but in that organism neither disruption of the Ran system nor disruption of HEH1 or HEH2 destabilizes the NE. The possibility that NE breakage in the *pim1-d1* mutant is caused by the inability to transport Lem2 to the INM is not consistent with our observations that NE breakage is significantly greater in *pim1-d1* cells than in  $\Delta$ *lem2* cells and that breakage in the  $\Delta$ *lem2* *pim1-d1* double mutant cells is significantly greater than that of the *pim1-d1* single mutant. These observations raise the possibility that another RanGTPase-dependent function is necessary for NE stability.

**Lem2 and Man1 anchor chromatin to the nuclear periphery via their HEH-domains.** In the animal cell lineage a HEH DNA-binding fold lies within the LEM domain of a subset of LAPs, and it interacts indirectly with DNA by binding to the animal cell specific DNA-binding protein BAF.<sup>19</sup> Phosphorylation, and perhaps other cell cycle dependent protein modifications of components of the lamina, releases chromatin from the NE at mitosis and promotes NEBD (reviewed in refs. 5, 17 and 18).

In single celled eukaryotes, which do not have BAF, the HEH domain has been predicted to bind directly to chromatin.<sup>19</sup> Consistent with this expectation, the Lem2- and Man1-dependent tethering of DNA to the NE depends on their HEH domains and excess HEH-domain peptide from either protein causes chromatin hypercompaction and the dissociation of chromatin from the nuclear periphery although the mechanism by which the interaction of Lem2 and Man1 with chromatin is modulated over the cell cycle remains unknown. However, interphase chromatin organization appears unchanged in the absence of *lem2*, *man1* or both suggesting that there may be other HEH-domain containing DNA binding proteins in *S. pombe*, although they cannot be identified by BLAST or psi-BLAST searches. Although the NE-localized fission yeast protein Ima1 does not have an HEH-domain, it may work in conjunction with Lem2 and Man1, because recent work shows that a triple null mutant of *lem2*, *man1* and *ima1* displays slow mitotic growth and nuclear envelope defects.<sup>68</sup>

The observation that chromatin associates with the overexpression-induced proliferated NE, specifically at the periphery of the Man1-induced “mini-nuclei” and the ability of excess HEH domain to release chromatin from the nuclear periphery, are consistent with a model in which Lem2 and Man1 anchor heterochromatin to the nuclear periphery. This possibility is consistent with the recent work from Karl Ekwall’s laboratory<sup>69</sup> showing that Man1 binds to multiple chromatin loci that are characterized by their association with the heterochromatin-specific binding protein Swi6. Man1 is associated with nearly 30% of the genome at loci that are distributed throughout the three *S. pombe* chromosomes including the centromere and subtelomeric regions. In these respects, Man1 functions similarly to the animal cell nuclear lamina in anchoring transcriptionally repressed genes to the nuclear periphery. It will be interesting to now determine the loci to which the Lem2 protein binds.

**Lem2 and Man1 anchor specific heterochromatic domains, including telomeres, to the NE.** *S. cerevisiae* Heh1 binds to telomeric and sub-telomeric repeats and when mutated changes the expression of a small number of sub-telomeric genes,<sup>39</sup> but does not alter the intranuclear distribution of telomeres (subtelomeric genes) or telomeric silencing, which is correlated with the NE association of telomeres in this organism.

Our preliminary data for Lem2 and the data of Karl Ekwall<sup>69</sup> for Man1 indicate that these two *S. pombe* proteins also bind to telomeric and sub-telomeric regions of the chromosomes. Although Lem2 and Man1 are not essential for global chromatin organization, they are each essential for telomere anchoring at the NE, a characteristic they share with the constitutive telomere-binding proteins Bqt3 and Bqt4.<sup>43</sup> Telomere distance from the NE increases in the absence of Bqt3 or Bqt4, but their distribution remains skewed toward the nuclear periphery, which suggested the possibility that other anchoring proteins exist, and Lem2 and Man1 are two such proteins.<sup>43</sup> In *S. pombe*, loss of telomeric nuclear envelope localization does not alter telomeric silencing or telomere length.<sup>43</sup>

Lem2, but neither Man1 nor the related Heh1 or Heh2 proteins of *S. cerevisiae*<sup>28,39</sup> (see Fig. 1A), accumulates at the SPB to which centromeric heterochromatin is anchored during interphase but not mitosis of the cell cycle, yet its SPB-specific function remains unknown: it does not influence mitotic chromosome segregation and although excess HEH-domain peptide dissociates chromatin from the nuclear periphery, it does not disrupt the interaction between the SPB and centromeric chromatin. Like Lem2, Ima1 is inner NE localized fission yeast

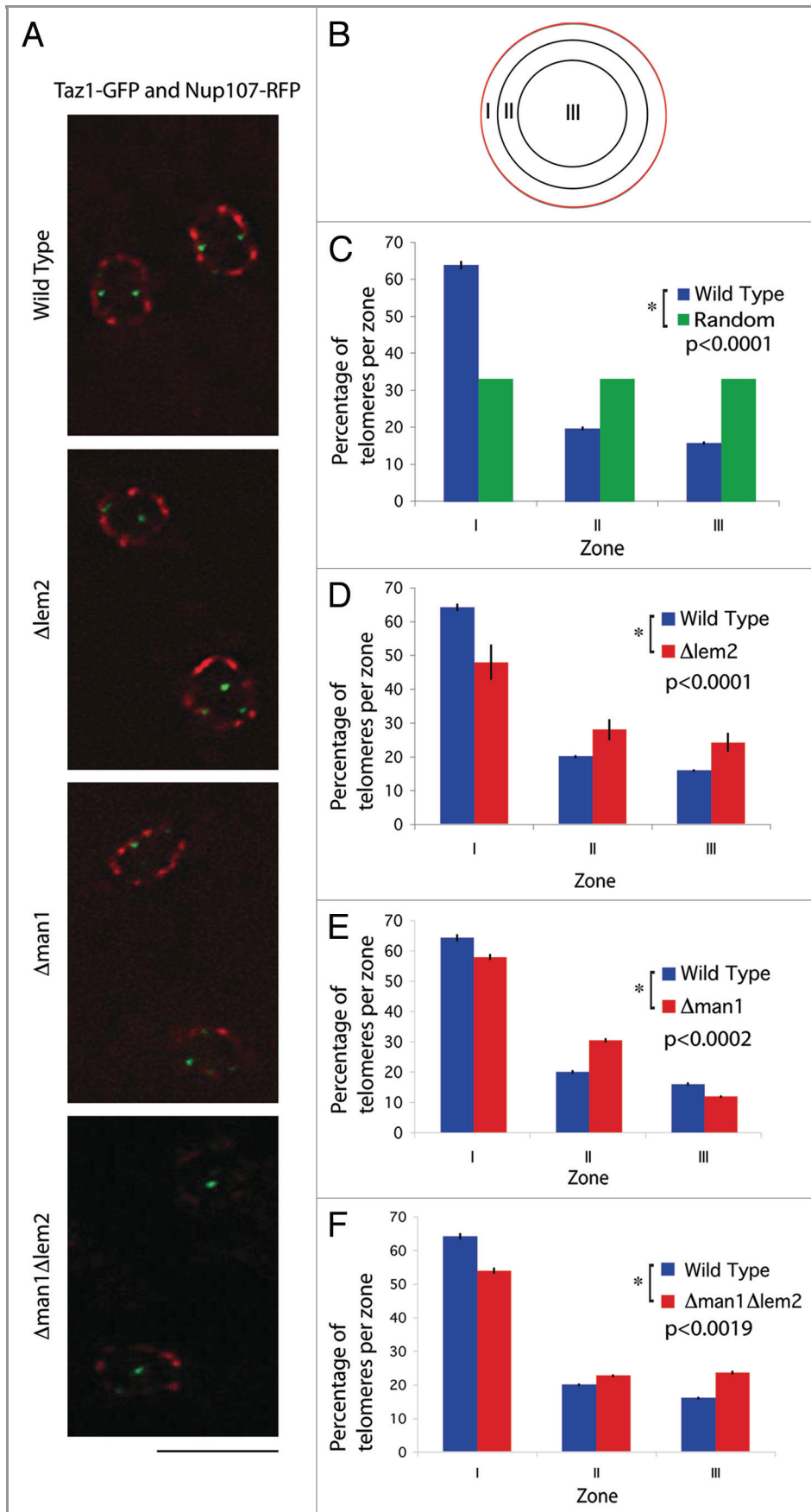


**Figure 6.** Lem2 and Man1 are each required for tethering telomeres to the nuclear periphery. (A) Wild type,  $\Delta$ lem2,  $\Delta$ man1 and  $\Delta$ man1 $\Delta$ lem2 cells with the telomere-binding protein Taz1-GFP (to visualize the telomere) and the NPC component Nup107-RFP (to visualize the nuclear periphery) were grown to log phase at 25°C in YE. Telomere localization within the nucleus relative to the nuclear periphery was monitored using deconvolution microscopy. Scale bar = 5  $\mu$ m. (B) Three zones of equal area were designated and each telomere was assigned to a zone based on its distance from the nuclear periphery relative to the nuclear diameter as previously described.<sup>58</sup> Zone I is the outermost layer representing telomeres at or near the nuclear periphery. Zone II is the intermediate layer, and zone III is the inner layer containing only telomeres near the center of the nucleus. (C–F) Comparison of percentage of telomeres found in each zone for wild type cells to (C) expected distribution of randomly distributed spots, (D)  $\Delta$ lem2 cells, (E)  $\Delta$ man1 cells and (F)  $\Delta$ man1 $\Delta$ lem2.  $n > 200$  for each strain. For comparative purposes, the same wild type distribution is shown in each graph. Asterisk indicates statistically significant difference between wild type and mutant distribution of telomeres calculated using the chi-square test.

protein enriched at the SPB,<sup>44,45</sup> but the SPB localization of these 2 proteins is mutually exclusive<sup>68</sup> suggesting that they may play distinct roles at the SPB which remain to be determined.

**Evolution of nuclear organization.** It has been proposed that proteins structurally related to Lem2 and Man1, with primitive HEH DNA binding folds and transmembrane domains, may have been present in the Last Eukaryotic Common Ancestor.<sup>19,70</sup> They may have played an important role in tethering nucleic acids to membranes at the time of emergence of the first eukaryote, thereby stabilizing these membranes. Our data indicate that the same may be true of *S. pombe* Lem2 and Man1. They influence nuclear structure and organization in the absence of two key components of the animal cell lamina: lamins, the intermediate filament proteins that form the NE scaffold, and BAF, the protein that mediates the binding of LEM-domain containing lamin-associated proteins to chromatin. Consistent with the possibility that HEH-domain containing proteins represent the foundation upon which the animal cell lamina was built, it has been postulated that the presence of the BAF protein in the animal cell lineage allowed for the proliferation and specialization of members of the LEM-domain protein family in animal cells.<sup>19</sup>

Comparative studies of nuclear organization in yeast, plants and animals will lead to a better understanding of the principles of nuclear organization as they relate to nuclear structure and function in both open and closed mitosis and to the evolution of nuclear organization since the emergence of the first nucleated cells.

## Materials and Methods

**Yeast cell culture.** Standard methods and genetic techniques were used<sup>71</sup> and strains are described in Table 1. Transformations were by lithium acetate.<sup>71,72</sup> Spotting experiments were performed by growing cells to mid-log phase and spotting 10<sup>6</sup> cells and 5-fold dilutions onto plates with the pink vital dye phloxine B (Sigma) that accumulates in dead cells, supplements and thiamine as indicated. DNA was visualized fixed cells using 4', 6-diamidino-2-phenylindole dihydrochloride (DAPI) or in live cells using Hoechst 33342 (Sigma-Aldrich). Gene expression, from the thiamine repressible *nmt1* gene promoter<sup>73</sup> in plasmids pREP3X,<sup>74</sup> pDUAL<sup>75</sup> or pDS473a,<sup>76</sup> was repressed by growth in EMM with 5mg/ml thiamine (promoter OFF), cells were grown under these conditions to mid-log phase, and then expression was derepressed by washing the culture and then incubating in supplemented EMM lacking thiamine (promoter ON) for 30 h to follow the consequent phenotype at 25°C unless otherwise noted. The conditions used for overexpressing proteins were the same for all experiments shown.

**Strain and plasmid construction.** To overexpress *man1* or *lem2*, the genes were PCR amplified from the *S. pombe* cDNA library  $\lambda$ ACT (generous gift from Steve Elledge). The product was digested with *XhoI* and *SmaI* or *Sall* and *SmaI*, and sub-cloned into pBluescript II SK (+) to create pBSK-*man1* or pBSK-*lem2*. The *XhoI-SmaI* insert of pBSK-*man1* was sub-cloned into the *XhoI-SmaI* sites of the multicopy plasmid pREP3X<sup>74</sup> (pREP3X-*man1*) and the *Sall-SmaI* insert of pBSK-*lem2* was

sub-cloned into the *Sall-SmaI* sites of pREP3X (pREP3X-*lem2*). The pDUAL-YFH1c vector,<sup>75</sup> expressing *man1* or *lem2* tagged at the C-terminus with YFP, FLAG and His6 from the *nmt1* promoter was integrated at the *leu1* locus by linearizing the DNA using *NotI* and transforming it into haploid wild-type cells (SS446). To construct a pDUAL-YFH1c vector expressing *man1* or *lem2* tagged at the C-terminus with YFP, FLAG and His6 but lacking the HEH domain ( $\Delta$ HEH) as previously defined,<sup>19</sup> inverse PCR of plasmids containing the full length genes (pDUAL-*lem2*, pDUAL-*man1*) was used to generate the internal deletion<sup>77</sup> of the HEH domain from *lem2* (nucleotides 16–147) and *man1* (nucleotides 22–153). *man1* <sup>$\Delta$ HEH</sup> or *lem2* <sup>$\Delta$ HEH</sup> were cloned between the *NheI-NruI* and *NheI-NdeI* sites, respectively, of the pDUAL-YFH1c<sup>75</sup> plasmid. To overexpress just the HEH domain of *man1* (nucleotides 1–153) or *lem2* (nucleotides 1–147), each domain was PCR amplified from the *S. pombe* cDNA library  $\lambda$ ACT (generous gift of Dr. Steve Elledge), the products digested with *BamHI* and *SmaI* and cloned into the multicopy pDS473a<sup>76</sup> plasmid.

To construct C-terminal GFP-tagged versions of *man1* or *lem2* at their chromosomal loci, the C-terminal domain was PCR amplified and cloned between the *BamHI-SmaI* sites of the pFA6aGFP-kanMX6<sup>78</sup> plasmid. The resulting plasmid was linearized using the *NheI* site in the C-terminal domain of *man1* or *lem2* and transformed into haploid wild-type cells (SS446).

The  $\Delta$ man1 (*man1* null) and  $\Delta$ lem2 (*lem2* null) strains were generated by PCR-based targeted gene replacement of the open reading frame with a KanMX4 drug resistance cassette<sup>78</sup> and identified by their ability to grow on YE plates with GIBCO™ Geneticin (G418) (Invitrogen).

**Fluorescence microscopy.** A DeltaVision Deconvolution Microscope System (Applied Precision, Issaquah, Wash.), with a Nikon TE200 inverted microscope and a Nikon Plan APO 100X 1.4 N.A. lens and a Photometrics CoolSnap HQ Camera (Roper Scientific) was used to collect images of the whole cell, by analyzing stacks of 0.2  $\mu$ m Z sections, that were projected two dimensionally using the maximum intensity protocol, using SoftWoRx3.3 (Applied Precision, Inc.) software. In some cases, as indicated, cells were examined using a Zeiss Axioskop fluorescence microscope, with a Zeiss Plan-NEO FLUAR 100X 1.3 N.A. lens, from which images were captured by a DVD 1300 Black and White CCD camera using QED software (Media Cybernetics). Individual images were extracted into Photoshop (Adobe) to generate the panels for the figures.

Live cells producing the NE localized NPC component Nsp1p fused to GFP (GFP-Nsp1p) to visualize the nuclear periphery and the soluble protein  $\beta$ -galactosidase fused to GFP and targeted to the nucleus by the SV40 nuclear localization signal (SV40 NLS-GFP- $\beta$ -gal) were used to visualize the nuclear interior and monitor NE integrity, as previously described.<sup>50</sup> In cells with intact NEs these GFP signals are exclusively nuclear, but in cells with broken NEs the SV40 NLS-GFP- $\beta$ -gal signal localizes throughout the cell. The percent of cells with broken NEs was determined by counting at least 200 cells.

Telomere localization was determined by assigning each to one of 3 zones equal in area within the nucleus as previously described

**Table 1.** Strains used in this study

Strain Name	Genotype	Source
SS445	<i>h<sup>+</sup> leu1-32 ura4-D18 ade6-M210</i>	Our Stock
SS446	<i>h<sup>-</sup> leu1-32 ura4-D18 ade6-M210</i>	Our Stock
SS447	<i>h<sup>+</sup> leu1-32 ura4-D18 ade6-M216</i>	Our Stock
SS777	<i>h<sup>+</sup> pim1-d1 leu1-32 ura4-D18 int::pREP3X-SV40NLS-GFP-lacZ int::pREP82X-GFP-nsp1</i>	Our Stock
SS817	<i>h<sup>-</sup> leu1-32 ura4-D18 int::pREP82X-GFP-nsp1 int::pREP3X-SV40NLS-GFP-lacZ</i>	Our Stock
SS1942	<i>h<sup>-</sup> leu1-32, ura4-D18, ade6-M210 pDUAL-lem2-YFP</i>	This study
SS1947	<i>h<sup>+</sup> nup107-tomato::Natmx4 leu1-32, ura4-D18, ade6-M216</i>	Fred Chang
SS1974	<i>h<sup>-</sup> leu1-32 ura4-D18 int::pREP3X-SV40 NLS-GFP-lacZ int::pREP82X-GFP-nsp1 pREP3X</i>	This study
SS1975	<i>h<sup>-</sup> leu1-32 ura4-D18 int::pREP3X-SV40 NLS-GFP-lacZ int::pREP82X-GFP-nsp1 pREP3X-man1</i>	This study
SS1976	<i>h<sup>-</sup> leu1-32 ura4-D18 int::pREP3X-SV40 NLS-GFP-lacZ int::pREP82X-GFP-nsp1 pREP3X-lem2</i>	This study
SS1990	<i>h<sup>-</sup> leu1-32 ura4-D18 int::pREP82X-GFP-nsp1 pREP3X</i>	This study
SS1993	<i>h<sup>-</sup> leu1-32 ura4-D18 int::pREP82X-GFP-nsp1 pREP3X-man1</i>	This study
SS1996	<i>h<sup>-</sup> leu1-32 ura4-D18 int::pREP82X-GFP-nsp1 pREP3X-lem2</i>	This study
SS2035	<i>h<sup>+</sup> man1:: KanMX6 leu1-32, ura4-D18, ade6-M216</i>	This study
SS2036	<i>h<sup>+</sup> man1:: KanMX6 leu1-32, ura4-D18, ade6-M210</i>	This study
SS2037	<i>h<sup>+</sup> lem2:: KanMX6 leu1-32, ura4-D18, ade6-M216</i>	This study
SS2040	<i>h<sup>+</sup> man1::14KanMX6 lem2::18KanMX6 leu1-23 ura4-D18 ade6-m216</i>	This study
SS2042	<i>h<sup>+</sup> lem2:: KanMX6 leu1-32, ura4-D18, ade6-M210 int::pREP3X-SV40 NLS-GFP-lacZ int::pREP82X-GFP-nsp1</i>	This study
SS2045	<i>int::pREP82X-GFP-nsp1</i>	This study
SS2046	<i>h<sup>-</sup> leu1-32, ura4-D18, ade6-M216 pREP3X</i>	This study
SS2047	<i>h<sup>-</sup> leu1-32, ura4-D18, ade6-M216 pREP3X-man1</i>	This study
SS2048	<i>h<sup>-</sup> leu1-32, ura4-D18, ade6-M216 pREP3X-lem2</i>	This study
SS2058	<i>h<sup>+</sup> pcp1.RFP:kan<sup>R</sup> ura4-D18</i>	This study
SS2089	<i>h<sup>+</sup> man1:: KanMX6 leu1-32, ura4-D18, ade6-M210 int::pREP3X-SV40NLS-GFP-lacZ int::pREP82X-GFP-nsp1</i>	This study
SS2090	<i>h<sup>+</sup> man1:: KanMX6 pim1-d1 leu1-32, ura4-D18 int::pREP3X-SV40NLS-GFP-lacZ int::pREP82X-GFP-nsp1</i>	This study
SS2126	<i>h<sup>-</sup> lem2-GFP::KanMX6 leu1-32, ura4-D18, ade6-M210</i>	This study
SS2127	<i>h<sup>-</sup> man1-GFP::KanMX6 leu1-32, ura4-D18, ade6-M210</i>	This study
SS2159	<i>h<sup>-</sup> lem2-GFP::KanMX6 pcp1.RFP:kan<sup>R</sup> leu1-32, ura4-D18</i>	This study
SS2169	<i>h<sup>+</sup> lem2:: KanMX6 leu1-32, ura4-D18, ade6-M210 int::pREP3X-SV40NLS-GFP-lacZ int::pREP82X-GFP-nsp1 pREP3X</i>	This study
SS2170	<i>h<sup>-</sup> man1:: KanMX6 leu1-32, ura4-D18, ade6-M210 int::pREP3X-SV40NLS-GFP-lacZ int::pREP82X-GFP-nsp1 pREP3X-lem2</i>	This study

**Table 1.** Strains used in this study (continued)

Strain Name	Genotype	Source
SS2171	<i>h<sup>+</sup> lem2:: KanMX6 leu1-32, ura4-D18, ade6-M210 int::pREP3X-SV40NLS-GFP-lacZ int::pREP82X-GFP-nsp1 pREP3X-man1</i>	This study
SS2172	<i>h<sup>-</sup> man1:: KanMX6 leu1-32, ura4-D18, ade6-M210 int::pREP3X-SV40NLS-GFP-lacZ int::pREP82X-GFP-nsp1 pREP3X-man1</i>	This study
SS2173	<i>h<sup>+</sup> lem2:: KanMX6 leu1-32, ura4-D18, ade6-M210 int::pREP3X-SV40NLS-GFP-lacZ int::pREP82X-GFP-nsp1 pREP3X-lem2</i>	This study
SS2192	<i>h<sup>-</sup> lem2-GFP::KanMX6 leu1-32, ura4-D18, ade6-M210 pREP3X</i>	This study
SS2193	<i>h<sup>-</sup> lem2-GFP::KanMX6 leu1-32, ura4-D18, ade6-M210 pREP3X-man1</i>	This study
SS2194	<i>h<sup>-</sup> lem2-GFP::KanMX6 leu1-32, ura4-D18, ade6-M210 pREP3X-lem2</i>	This study
SS2198	<i>h<sup>-</sup> man1-GFP::KanMX6 leu1-32, ura4-D18, ade6-M210 pREP3X</i>	This study
SS2199	<i>h<sup>-</sup> man1-GFP::KanMX6 leu1-32, ura4-D18, ade6-M210 pREP3X-man1</i>	This study
SS2200	<i>h<sup>-</sup> man1-GFP::KanMx leu1-32, ura4-D18, ade6-M210 pREP3X-lem2</i>	This study
SS2234	<i>h<sup>-</sup> leu1-32, ura4-D18, ade6-M210 pDUAL-man1-YFP</i>	This study
SS2236	<i>h<sup>-</sup> leu1-32, ura4-D18, ade6-M210 pDUAL-man1<sup>ΔHEH</sup>-YFP</i>	This study
SS2268	<i>h<sup>-</sup> leu1-32, ura4-D18, ade6-M210 pDUAL-lem2<sup>ΔHEH</sup>-YFP</i>	This study
SS2306	<i>h<sup>+</sup> man1::NatMX4 leu1-32, ura4-D18, ade6-M216</i>	This study
SS2343	<i>h<sup>+</sup> lem2::NatMX4 leu1-32, ura4-D18, ade6-M210</i>	This study
SS2352	<i>h<sup>-</sup> taz1-GFP:: KanMX6 leu1-32, ura4-D18, ade6-M216</i>	This study
SS2357	<i>h<sup>-</sup> taz1-GFP:: KanMX6 lem2::Natmx4 leu1-32, ura4-D18, ade6-M216</i>	This study
SS2358	<i>h<sup>-</sup> taz1-GFP:: KanMX6 man1::Natmx4 leu1-32, ura4-D18, ade6-M216</i>	This study
SS2394	<i>h<sup>+</sup> nup107-tomato::NatMX4 leu1-32, ura4-D18, ade6-M216 pDS473a</i>	This Study
SS2395	<i>h<sup>+</sup> nup107-tomato::NatMX4 leu1-32, ura4-D18, ade6-M216 pDS473a-HEH<sup>lem2</sup></i>	This Study
SS2396	<i>h<sup>+</sup> nup107-tomato::NatMX4 leu1-32, ura4-D18, ade6-M216 pDS473a-HEH<sup>man1</sup></i>	This Study
SS2407	<i>h<sup>+</sup> leu1-32, ura4-D18, ade6-M210 pDS473a</i>	This Study
SS2408	<i>h<sup>+</sup> leu1-32, ura4-D18, ade6-M210 pDS473a-HEH<sup>man1</sup></i>	This Study
SS2409	<i>h<sup>+</sup> leu1-32, ura4-D18, ade6-M210 pDS473a-HEH<sup>lem2</sup></i>	This Study
SS2410	<i>h<sup>-</sup> sid4-GFP:: KanMX6 leu1-32, ura4-D18, ade6-M210 pDS473a</i>	This Study
SS2411	<i>h<sup>-</sup> sid4-GFP:: KanMX6 leu1-32, ura4-D18, ade6-M210 pDS473a-HEH<sup>man1</sup></i>	This Study
SS2412	<i>h<sup>-</sup> sid4-GFP:: KanMX6 leu1-32, ura4-D18, ade6-M210 pDS473a-HEH<sup>lem2</sup></i>	This Study
SS2418	<i>h<sup>-</sup> nup107-tomato::NatMX4 taz1-GFP::KanMX6 leu1-32, ura4-D18, ade6-M216</i>	This Study
SS2420	<i>h<sup>+</sup> nup107-tomato::NatMX4 taz1-GFP::KanMX6 lem2:: NatMX4 leu1-32, ura4-D18, ade6-M216</i>	This Study

**Table 1.** Strains used in this study (continued)

Strain Name	Genotype	Source
SS2425	<i>h<sup>-</sup> nup107-tomato::NatMX4 taz1-GFP::KanMX6 man1::NatMX4 leu1-32, ura4-D18, ade6-M216</i>	This Study
SS2565	<i>h- man1::Kan lem2::Nat int::pREP3X-SV40 NLS-GFP-lacZ int::pREP82X-GFP-nsp1 leu1-32 ura4-D18 ade6-m210</i>	This Study
SS2566	<i>h- man1::Kan lem2::Nat int::pREP3X-SV40 NLS-GFP-lacZ int::pREP82X-GFP-nsp1 leu1-32 ura4-D18 ade6-m210</i>	This Study
SS2628	<i>h+ pim1-d1 man1::Kan lem2::Nat int::pREP3X-SV40 NLS-GFP-lacZ int::pREP82X-GFP-nsp1 leu1-32 ura4-D18 ade6-m210</i>	This Study
SS2635	<i>h- nup107-tomato::NatMX4 taz1-GFP::KanMX6 man1::NatMX4 lem2::KanMX6 leu1-32 ura4-D18 ade6-m216</i>	This Study

in *S. cerevisiae*<sup>58</sup> except that: the *S. pombe* telomeres were localized with Taz1-GFP; the nuclear pores were visualized with Nup107-RFP; live cells were grown in YE liquid cultures instead of on agar; and 20 stacks of images (exposure, 1,000 ms; step size, 200 nm) were taken using a deconvolution microscope instead of a wide-field microscope.

To monitor the fidelity of chromosome segregation, wild type,  $\Delta$ man1 and  $\Delta$ lem2 strains were constructed that carried a tandem array of 256 lac operator (lacO) repeats integrated at the *lys1<sup>+</sup>* locus that is tightly linked to the centromere of chromosome I, and expressed a LacI-GFP chimera that binds to the lacO repeats.<sup>53</sup> These strains were used to monitor chromosome segregation during mitosis, as previously described<sup>53</sup> by determining whether binucleated cells have one GFP dot in each nucleus (equal segregation) or two GFP dots in one nucleus and none in the other (mis-segregation).

**Electron microscopy.** Cells were harvested by vacuum filtration onto 0.45  $\mu$ m Millipore filters and the resulting wet cell paste was loaded into aluminum sample holders with a 100 or 200  $\mu$ m well (Technotrade International) for high pressure freezing in a

Bal-Tec HPM 010 (Leica, Inc.). Frozen samples were freeze-substituted in 2% osmium tetroxide and 0.1% uranyl acetate in acetone at  $-80^{\circ}\text{C}$  for 4 d, warmed to  $-20^{\circ}\text{C}$  overnight, then to  $4^{\circ}\text{C}$  for 3 hr and room temperature for 1 h, followed by infiltration and embedding in Epon/Araldite resin.<sup>79</sup> Thin sections (60–70 nm) were stained with 2% uranyl acetate dissolved in 70% methanol, 30% water, rinsed, and stained in lead citrate. Images were obtained with a Philips CM10 or CM100 (FEI, Inc., Hillsboro, OR) equipped with a Gatan Bioscan digital camera.

#### Disclosure of Potential Conflicts of Interest

The authors declare that they have no financial interests in relation to the submitted work.

#### Acknowledgments

We acknowledge the important contributions of Dr. Makoto Umeda to the initial characterization of *lem2*. We also thank him for **Figure 1B** and Nimrat Kaur for **Figure 1C**. We are grateful to Minoru Yoshida for providing information and strains prior to publication, Zac Cande, Julie Cooper, Fred Chang and Iain Hagan for strains, Dick McIntosh, Richard Atkinson and Xiangwei He for advice, Ilia Spiridonov, Katya Grishchuk and Dick McIntosh for help with EM sample preparation, Dr. Tom Giddings for EM, and Kristen Meerbrey, Brigitte Maillot and Heetae Jeong for strain construction, and Babet Steglich and Karl Ekwall for communicating results prior to publication. This material is based in part on work supported by the National Science Foundation under Grant numbers 0344471 and 0744945 (to S.S.). Any opinions, findings and conclusions or recommendations expressed in this article are those of the authors and do not necessarily reflect the views of the National Science Foundation. Y.G. was supported in part by National Institutes of Health grants IMSD R25 GM56929 and 5F31 GM 076862.

#### Supplemental Material

Supplemental material may be downloaded here: <http://www.landesbioscience.com/journals/nucleus/article/18824/>

#### References

- Voeltz GK, Prinz WA, Shibata Y, Rist JM, Rapoport TA. A class of membrane proteins shaping the tubular endoplasmic reticulum. *Cell* 2006; 124:573-86; PMID: 16469703; <http://dx.doi.org/10.1016/j.cell.2005.11.047>
- Hetzer MW, Walther TC, Mattaj IW. Pushing the envelope: structure, function, and dynamics of the nuclear periphery. *Annu Rev Cell Dev Biol* 2005; 21:347-80; PMID:16212499; <http://dx.doi.org/10.1146/annurev.cellbio.21.090704.151152>
- Anderson DJ, Hetzer MW. Reshaping of the endoplasmic reticulum limits the rate for nuclear envelope formation. *J Cell Biol* 2008; 182:911-24; PMID: 18779370; <http://dx.doi.org/10.1083/jcb.200805140>
- D'Angelo MA, Hetzer MW. The role of the nuclear envelope in cellular organization. *Cell Mol Life Sci* 2006; 63:316-32; PMID:16389459; <http://dx.doi.org/10.1007/s00018-005-5361-3>
- Gruenbaum Y, Margalit A, Goldman RD, Shumaker DK, Wilson KL. The nuclear lamina comes of age. *Nat Rev Mol Cell Biol* 2005; 6:21-31; PMID:15688064; <http://dx.doi.org/10.1038/nrm1550>
- Sazer S. Nuclear envelope: nuclear pore complexity. *Curr Biol* 2005; 15:R23-6; PMID:15649347; <http://dx.doi.org/10.1016/j.cub.2004.12.015>
- Ding R, West RR, Morpew DM, Oakley BR, McIntosh JR. The spindle pole body of *Schizosaccharomyces pombe* enters and leaves the nuclear envelope as the cell cycle proceeds. *Mol Biol Cell* 1997; 8:1461-79; PMID:9285819
- McIntosh JR, O'Toole ET. Life cycles of yeast spindle pole bodies: getting microtubules into a closed nucleus. *Biol Cell* 1999; 91:305-12; PMID:10518997; [http://dx.doi.org/10.1016/S0248-4900\(99\)80091-4](http://dx.doi.org/10.1016/S0248-4900(99)80091-4)
- McCully EK, Robinow CF. Mitosis in the fission yeast *Schizosaccharomyces pombe*: a comparative study with light and electron microscopy. *J Cell Sci* 1971; 9:475-507; PMID:4108061
- Cai M, Huang Y, Ghirlando R, Wilson KL, Craigie R, Clore GM. Solution structure of the constant region of nuclear envelope protein LAP2 reveals two LEM-domain structures: one binds BAF and the other binds DNA. *EMBO J* 2001; 20:4399-407; PMID:11500367; <http://dx.doi.org/10.1093/emboj/20.16.4399>
- Shumaker DK, Lee KK, Tanhehco YC, Craigie R, Wilson KL. LAP2 binds to BAF/DNA complexes: requirement for the LEM domain and modulation by variable regions. *EMBO J* 2001; 20:1754-64; PMID: 11285238; <http://dx.doi.org/10.1093/emboj/20.7.1754>
- Lee KK, Haraguchi T, Lee RS, Koujin T, Hiraoka Y, Wilson KL. Distinct functional domains in emerin bind lamin A and DNA-bridging protein BAF. *J Cell Sci* 2001; 114:4567-73; PMID:11792821
- Wiesel N, Mattout A, Melcer S, Melamed-Book N, Herrmann H, Medalia O, et al. Laminopathic mutations interfere with the assembly, localization, and dynamics of nuclear lamins. *Proc Natl Acad Sci USA* 2008; 105:180-5; PMID:18162544; <http://dx.doi.org/10.1073/pnas.0708974105>
- Worman HJ, Fong LG, Muchir A, Young SG. Laminopathies and the long strange trip from basic cell biology to therapy. *J Clin Invest* 2009; 119:1825-36; PMID:19587457; <http://dx.doi.org/10.1172/JCI37679>

15. Burke B, Stewart CL. The laminopathies: the functional architecture of the nucleus and its contribution to disease. *Annu Rev Genomics Hum Genet* 2006; 7:369-405; PMID:16824021; <http://dx.doi.org/10.1146/annurev.genom.7.080505.115732>
16. Kim Y, Sharov AA, McDole K, Cheng M, Hao H, Fan CM, et al. Mouse B-Type Lamins Are Required for Proper Organogenesis But Not by Embryonic Stem Cells. *Science* 2011; PMID:22116031; <http://dx.doi.org/10.1126/science.1211222>
17. Hirano Y, Iwase Y, Ishii K, Kumeta M, Horigome T, Takeyasu K. Cell cycle-dependent phosphorylation of MAN1. *Biochemistry* 2009; 48:1636-43; PMID:19166343; <http://dx.doi.org/10.1021/bi802060v>
18. Hirano Y, Segawa M, Ouchi FS, Yamakawa Y, Furukawa K, Takeyasu K, et al. Dissociation of emerin from barrier-to-autointegration factor is regulated through mitotic phosphorylation of emerin in a xenopus egg cell-free system. *J Biol Chem* 2005; 280:39925-33; PMID:16204256; <http://dx.doi.org/10.1074/jbc.M503214200>
19. Mans BJ, Anantharaman V, Aravind L, Koonin E. Comparative genomics, evolution and origins of the nuclear envelope and nuclear pore complex. *Cell Cycle* 2004; 3:1612-37; PMID:15611647; <http://dx.doi.org/10.4161/cc.3.12.1316>
20. Meier I, Zhou X, Brkljacic J, Rose A, Zhao Q, Xu XM. Targeting proteins to the plant nuclear envelope. *Biochem Soc Trans* 2010; 38:733-40; PMID:20491658; <http://dx.doi.org/10.1042/BST0380733>
21. Mattaj IW. Sorting out the nuclear envelope from the endoplasmic reticulum. *Nat Rev Mol Cell Biol* 2004; 5:65-9; PMID:14663490; <http://dx.doi.org/10.1038/nrm1263>
22. Shibata Y, Voeltz GK, Rapoport TA. Rough sheets and smooth tubules. *Cell* 2006; 126:435-9; PMID:16901774; <http://dx.doi.org/10.1016/j.cell.2006.07.019>
23. Anderson DJ, Hetzer MW. Nuclear envelope formation by chromatin-mediated reorganization of the endoplasmic reticulum. *Nat Cell Biol* 2007; 9:1160-6; PMID:17828249; <http://dx.doi.org/10.1038/ncb1636>
24. Anderson DJ, Vargas JD, Hsiao JP, Hetzer MW. Recruitment of functionally distinct membrane proteins to chromatin mediates nuclear envelope formation in vivo. *J Cell Biol* 2009; 186:183-91; PMID:19620630; <http://dx.doi.org/10.1083/jcb.200901106>
25. Lim HWG, Huber G, Torii Y, Hirata A, Miller J, Sazer S. Vesicle-like biomechanics governs important aspects of nuclear geometry in fission yeast. *PLoS ONE* 2007; 2:e948; PMID:17895989; <http://dx.doi.org/10.1371/journal.pone.0000948>
26. Gonzalez Y, Meerbrey K, Chong J, Torii Y, Padte NN, Sazer S. Nuclear shape, growth and integrity in the closed mitosis of fission yeast depend on the Ran-GTPase system, the spindle pole body and the endoplasmic reticulum. *J Cell Sci* 2009; 122:2464-72; PMID:19571115; <http://dx.doi.org/10.1242/jcs.049999>
27. Demeter J, Morpheus M, Sazer S. A mutation in the RCC1-related protein pim1 results in nuclear envelope fragmentation in fission yeast. *Proc Natl Acad Sci USA* 1995; 92:1436-40; PMID:7877997; <http://dx.doi.org/10.1073/pnas.92.5.1436>
28. King MC, Lusk CP, Blobel G. Karyopherin-mediated import of integral inner nuclear membrane proteins. *Nature* 2006; 442:1003-7; PMID:16929305; <http://dx.doi.org/10.1038/nature05075>
29. Ohba T, Schirmer EC, Nishimoto T, Gerace L. Energy- and temperature-dependent transport of integral proteins to the inner nuclear membrane via the nuclear pore. *J Cell Biol* 2004; 167:1051-62; PMID:15611332; <http://dx.doi.org/10.1083/jcb.200409149>
30. Misteli T. Beyond the sequence: cellular organization of genome function. *Cell* 2007; 128:787-800; PMID:17320514; <http://dx.doi.org/10.1016/j.cell.2007.01.028>
31. Cremer T, Cremer M. Chromosome territories. *Cold Spring Harb Perspect Biol* 2010; 2:a003889; PMID:20300217; <http://dx.doi.org/10.1101/cshperspect.a003889>
32. Taddei A, Hediger F, Neumann FR, Gasser SM. The function of nuclear architecture: a genetic approach. *Annu Rev Genet* 2004; 38:305-45; PMID:15568979; <http://dx.doi.org/10.1146/annurev.genet.37.110801.142705>
33. Goffeau A, Barrell BG, Bussey H, Davis RW, Dujon B, Feldmann H, et al. Life with 6000 genes. *Science* 1996; 274:546-7; PMID:8849441; <http://dx.doi.org/10.1126/science.274.5287.546>
34. Eisen JA, Wood V, Gwilliam R, Rajandream MA, Lyne M, Lyne R, et al. The genome sequence of *Schizosaccharomyces pombe*. *Nature* 2002; 415:845-8; PMID:11859347; <http://dx.doi.org/10.1038/nature725>
35. Lusk CP, Blobel G, King MC. Highway to the inner nuclear membrane: rules for the road. *Nat Rev Mol Cell Biol* 2007; 8:414-20; PMID:17440484; <http://dx.doi.org/10.1038/nrm2165>
36. Huh WK, Falvo JV, Gerke LC, Carroll AS, Howson RW, Weissman JS, et al. Global analysis of protein localization in budding yeast. *Nature* 2003; 425:686-91; PMID:14562095; <http://dx.doi.org/10.1038/nature02026>
37. Matsuyama A, Arai R, Yashiroda Y, Shirai A, Kamata A, Sekido S, et al. ORFeome cloning and global analysis of protein localization in the fission yeast *Schizosaccharomyces pombe*. *Nat Biotechnol* 2006; 24:841-7; PMID:16823372; <http://dx.doi.org/10.1038/nbt1222>
38. Cam HP, Sugiyama T, Chen ES, Chen X, FitzGerald PC, Grewal SI. Comprehensive analysis of heterochromatin- and RNAi-mediated epigenetic control of the fission yeast genome. *Nat Genet* 2005; 37:809-19; PMID:15976807; <http://dx.doi.org/10.1038/ng1602>
39. Grund SE, Fischer T, Cabal GG, Antunez O, Perez-Ortin JE, Hurr E. The inner nuclear membrane protein Src1 associates with subtelomeric genes and alters their regulated gene expression. *J Cell Biol* 2008; 182:897-910; PMID:18762579; <http://dx.doi.org/10.1083/jcb.200803098>
40. Mekhail K, Seebacher J, Gygi SP, Moazed D. Role for perinuclear chromosome tethering in maintenance of genome stability. *Nature* 2008; 456:667-70; PMID:18997772; <http://dx.doi.org/10.1038/nature07460>
41. Goto B, Okazaki K, Niwa O. Cytoplasmic microtubular system implicated in de novo formation of a Rab1-like orientation of chromosomes in fission yeast. *J Cell Sci* 2001; 114:2427-35; PMID:11559751
42. Funabiki H, Hagan I, Uzawa S, Yanagida M. Cell cycle-dependent specific positioning and clustering of centromeres and telomeres in fission yeast. *J Cell Biol* 1993; 121:961-76; PMID:8388878; <http://dx.doi.org/10.1083/jcb.121.5.961>
43. Chikashige Y, Yamane M, Okamasu K, Tsutsumi C, Kojidani T, Sato M, et al. Membrane proteins Bqt3 and -4 anchor telomeres to the nuclear envelope to ensure chromosomal bouquet formation. *J Cell Biol* 2009; 187:413-27; PMID:19948484; <http://dx.doi.org/10.1083/jcb.200902122>
44. Hayashi A, Da-Qiao D, Tsutsumi C, Chikashige Y, Masuda H, Haraguchi T, et al. Localization of gene products using a chromosomally tagged GFP-fusion library in the fission yeast *Schizosaccharomyces pombe*. *Genes Cells* 2009; 14:217-25; PMID:19170768; <http://dx.doi.org/10.1111/j.1365-2443.2008.01264.x>
45. King MC, Drivas TG, Blobel G. A network of nuclear envelope membrane proteins linking centromeres to microtubules. *Cell* 2008; 134:427-38; PMID:18692466; <http://dx.doi.org/10.1016/j.cell.2008.06.022>
46. Prifert K, Vogel A, Krohne G. The lamin CxxM motif promotes nuclear membrane growth. *J Cell Sci* 2004; 117:6105-16; PMID:15546914; <http://dx.doi.org/10.1242/jcs.01532>
47. Ralle T, Grund C, Franke WW, Stick R. Intranuclear membrane structure formations by CaaX-containing nuclear proteins. *J Cell Sci* 2004; 117:6095-104; PMID:15546917; <http://dx.doi.org/10.1242/jcs.01528>
48. Finn RD, Mistry J, Tate J, Coghill P, Heger A, Pollington JE, et al. The Pfam protein families database. *Nucleic Acids Res* 2010; 38:D211-22; PMID:19920124; <http://dx.doi.org/10.1093/nar/gkp985>
49. Caputo S, Couprie J, Duband-Goulet I, Konde E, Lin F, Braud S, et al. The carboxyl-terminal nucleoplasmic region of MAN1 exhibits a DNA binding winged helix domain. *J Biol Chem* 2006; 281:18208-15; PMID:16648637; <http://dx.doi.org/10.1074/jbc.M601980200>
50. Yoshida M, Sazer S. Nucleocytoplasmic transport and nuclear envelope integrity in the fission yeast *Schizosaccharomyces pombe*. *Methods* 2004; 33:226-38; PMID:15157890; <http://dx.doi.org/10.1016/j.jmeth.2003.11.018>
51. Grallert A, Krapp A, Bagley S, Simanis V, Hagan IM. Recruitment of NIMA kinase shows that maturation of the *S. pombe* spindle-pole body occurs over consecutive cell cycles and reveals a role for NIMA in modulating SIN activity. *Genes Dev* 2004; 18:1007-21; PMID:15132994; <http://dx.doi.org/10.1101/gad.296204>
52. Miki F, Kurabayashi A, Tange Y, Okazaki K, Shimanuki M, Niwa O. Two-hybrid search for proteins that interact with Sad1 and Kms1, two membrane-bound components of the spindle pole body in fission yeast. *Mol Genet Genomics* 2004; 270:449-61; PMID:14655046; <http://dx.doi.org/10.1007/s00438-003-0938-8>
53. Nabeshima K, Nakagawa T, Straight AF, Murray A, Chikashige Y, Yamashita YM, et al. Dynamics of centromeres during metaphase-anaphase transition in fission yeast: Dis1 is implicated in force balance in metaphase bipolar spindle. *Mol Biol Cell* 1998; 9:3211-25; PMID:9802907
54. Wright R, Basson M, D'Ari L, Rine J. Increased amounts of HMG-CoA reductase induce "karmellae": a proliferation of stacked membrane pairs surrounding the yeast nucleus. *J Cell Biol* 1988; 107:101-14; PMID:3292536; <http://dx.doi.org/10.1083/jcb.107.1.101>
55. Pidoux AL, Armstrong J. The BiP protein and the endoplasmic reticulum of *Schizosaccharomyces pombe*: fate of the nuclear envelope during cell division. *J Cell Sci* 1993; 105:1115-20; PMID:8227200
56. Tomlin GC, Morrell JL, Gould KL. The spindle pole body protein Cdc1p links Sid4p to the fission yeast septation initiation network. *Mol Biol Cell* 2002; 13:1203-14; PMID:11950932; <http://dx.doi.org/10.1091/mbc.01-09-0455>
57. Jin Y, Uzawa S, Cande WZ. Fission yeast mutants affecting telomere clustering and meiosis-specific spindle pole body integrity. *Genetics* 2002; 160:861-76; PMID:11901107
58. Hediger F, Taddei A, Neumann FR, Gasser SM. Methods for visualizing chromatin dynamics in living yeast. *Methods Enzymol* 2004; 375:345-65; PMID:14870677; [http://dx.doi.org/10.1016/S0076-6879\(03\)75022-8](http://dx.doi.org/10.1016/S0076-6879(03)75022-8)
59. Ma Y, Cai S, Lv Q, Jiang Q, Zhang Q, Sodmergen, et al. Lamin B receptor plays a role in stimulating nuclear envelope production and targeting membrane vesicles to chromatin during nuclear envelope assembly through direct interaction with importin beta. *J Cell Sci* 2007; 120:520-30; PMID:17251381; <http://dx.doi.org/10.1242/jcs.03355>
60. Smith S, Blobel G. Colocalization of vertebrate lamin B and lamin B receptor (LBR) in nuclear envelopes and in LBR-induced membrane stacks of the yeast *Saccharomyces cerevisiae*. *Proc Natl Acad Sci USA* 1994; 91:10124-8; PMID:7937849; <http://dx.doi.org/10.1073/pnas.91.21.10124>
61. Hattier T, Andrusis ED, Tartakoff AM. Immobility, inheritance and plasticity of shape of the yeast nucleus. *BMC Cell Biol* 2007; 8:47; PMID:17996101; <http://dx.doi.org/10.1186/1471-2121-8-47>

62. Schirmer EC, Guan T, Gerace L. Involvement of the lamin rod domain in heterotypic lamin interactions important for nuclear organization. *J Cell Biol* 2001; 153:479-89; PMID:11331300; <http://dx.doi.org/10.1083/jcb.153.3.479>
63. Goldman RD, Shumaker DK, Erdos MR, Eriksson M, Goldman AE, Gordon LB, et al. Accumulation of mutant lamin A causes progressive changes in nuclear architecture in Hutchinson-Gilford progeria syndrome. *Proc Natl Acad Sci USA* 2004; 101:8963-8; PMID:15184648; <http://dx.doi.org/10.1073/pnas.0402943101>
64. Campbell JL, Lorenz A, Witkin KL, Hays T, Loidl J, Cohen-Fix O. Yeast nuclear envelope subdomains with distinct abilities to resist membrane expansion. *Mol Biol Cell* 2006; 17:1768-78; PMID:16467382; <http://dx.doi.org/10.1091/mbc.E05-09-0839>
65. Yewdell WT, Colombi P, Makhnevych T, Lusk CP. Luminal interactions in nuclear pore complex assembly and stability. *Mol Biol Cell* 2011; 22:1375-88; PMID:21346187; <http://dx.doi.org/10.1091/mbc.E10-06-0554>
66. Tallada VA, Tanaka K, Yanagida M, Hagan IM. The *S. pombe* mitotic regulator Cut12 promotes spindle pole body activation and integration into the nuclear envelope. *J Cell Biol* 2009; 185:875-88; PMID:19487457; <http://dx.doi.org/10.1083/jcb.200812108>
67. Sazer S, Nurse P. A fission yeast RCC1-related protein is required for the mitosis to interphase transition. *EMBO J* 1994; 13:606-15; PMID:8313905
68. Hiraoka Y, Maekawa H, Asakawa H, Chikashige Y, Kojidani T, Osakada H, et al. Inner Nuclear Membrane Protein Ima1 is Dispensable for Intranuclear Positioning of Centromeres. *Genes Cells* 2011; 16:1000-11; PMID:21880100; <http://dx.doi.org/10.1111/j.1365-2443.2011.01544.x>
69. Steglich B, Filion G, van Steensel B, Ekwall K. The inner nuclear membrane proteins Man1 and Ima1 link to two different types of chromatin at the nuclear periphery in *S. pombe*. *Nucleus* 2012; 3:78-88; PMID:22156748; <http://dx.doi.org/10.4161/nucl.3.1.18825>
70. Wilson KL, Dawson SC. Evolution: functional evolution of nuclear structure. *J Cell Biol* 2011; 195:171-81; PMID:22006947; <http://dx.doi.org/10.1083/jcb.201103171>
71. Moreno S, Klar A, Nurse P. Molecular genetic analysis of fission yeast *Schizosaccharomyces pombe*. *Methods Enzymol* 1991; 194:795-823; PMID:2005825; [http://dx.doi.org/10.1016/0076-6879\(91\)94059-L](http://dx.doi.org/10.1016/0076-6879(91)94059-L)
72. Suga M, Hatakeyama T. A rapid and simple procedure for high-efficiency lithium acetate transformation of cryopreserved *Schizosaccharomyces pombe* cells. *Yeast* 2005; 22:799-804; PMID:16088874; <http://dx.doi.org/10.1002/yea.1247>
73. Maundrell K. nmt1 of fission yeast. *J Biol Chem* 1990; 265:10857-64; PMID:2358444
74. Forsburg SL. Comparison of *Schizosaccharomyces pombe* expression systems. *Nucleic Acids Res* 1993; 21:2955-56; PMID:8332516; <http://dx.doi.org/10.1093/nar/21.12.2955>
75. Matsuyama A, Shirai A, Yashiroda Y, Kamata A, Horinouchi S, Yoshida M. pDUAL, a multipurpose, multicopy vector capable of chromosomal integration in fission yeast. *Yeast* 2004; 21:1289-305; PMID:15546162; <http://dx.doi.org/10.1002/yea.1181>
76. Forsburg SL, Sherman DA. General purpose tagging vectors for fission yeast. *Gene* 1997; 191:191-5; PMID:9218719; [http://dx.doi.org/10.1016/S0378-1119\(97\)00058-9](http://dx.doi.org/10.1016/S0378-1119(97)00058-9)
77. Xu Y, Gong Z. Adaptation of inverse PCR to generate an internal deletion. *Biotechniques* 1999; 26:639-41; PMID:10343901
78. Bähler J, Wu JQ, Longtrine MS, Shah NG, McKenzie A. 3rd, Steever AB, et al. Heterologous modules for efficient and versatile PCR-based gene targeting in *Schizosaccharomyces pombe*. *Yeast* 1998; 14:943-51; PMID:9717240; [http://dx.doi.org/10.1002/\(SICI\)1097-0061\(199807\)14:10<943::AID-YEA292>3.0.CO;2-Y](http://dx.doi.org/10.1002/(SICI)1097-0061(199807)14:10<943::AID-YEA292>3.0.CO;2-Y)
79. Giddings TH, Jr., O'Toole ET, Morphey M, Mastronarde DN, McIntosh JR, Winey M. Using rapid freeze and freeze-substitution for the preparation of yeast cells for electron microscopy and three-dimensional analysis. *Methods Cell Biol* 2001; 67:27-42; PMID:11550475; [http://dx.doi.org/10.1016/S0091-679X\(01\)67003-1](http://dx.doi.org/10.1016/S0091-679X(01)67003-1)

Landes Bioscience.

Do not distribute.